

Figure 14.1
 Seeing two-dimensional objects in flatland.
 (a) With a central perspective;
 (b) under parallel projection.

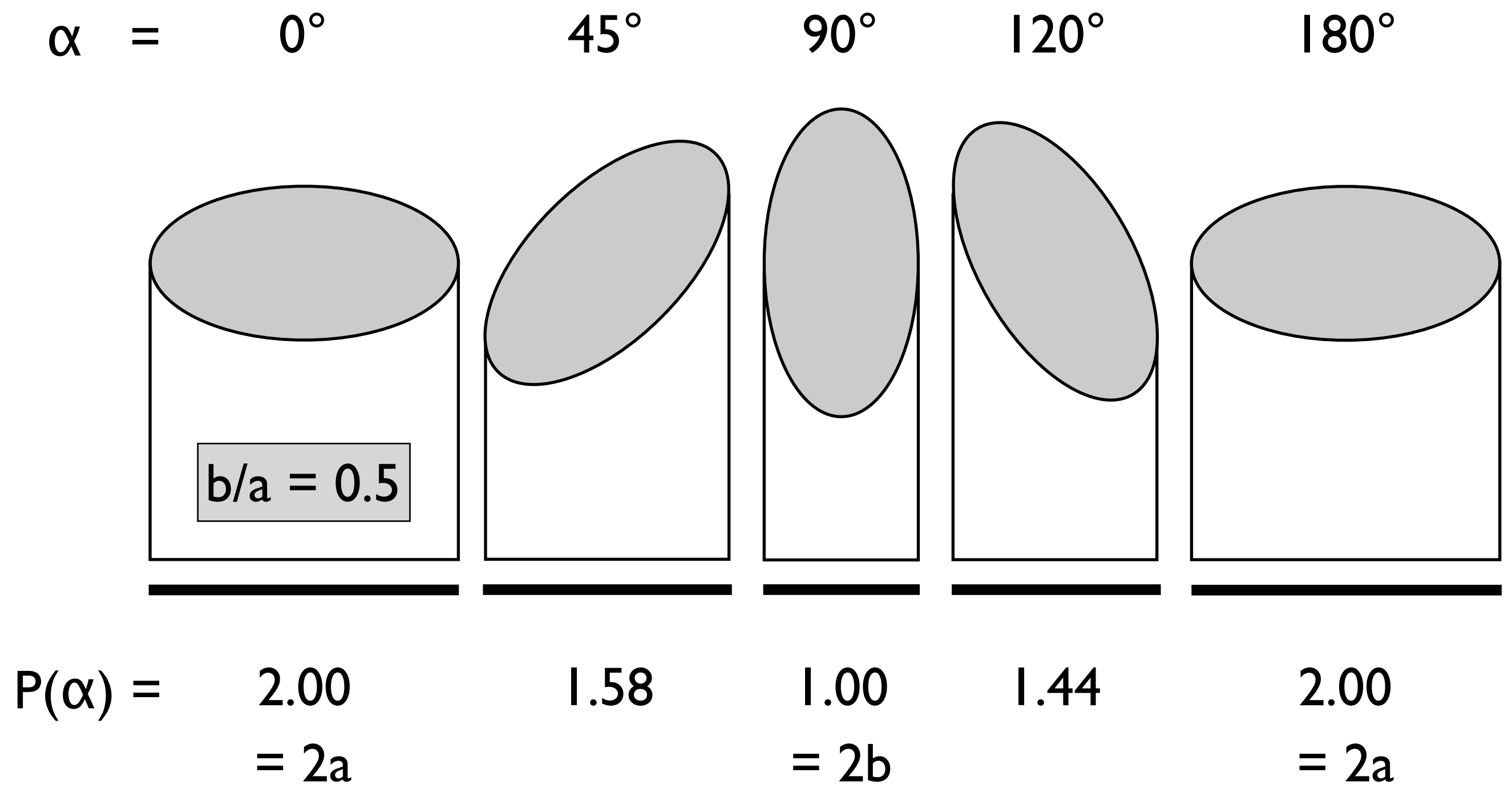
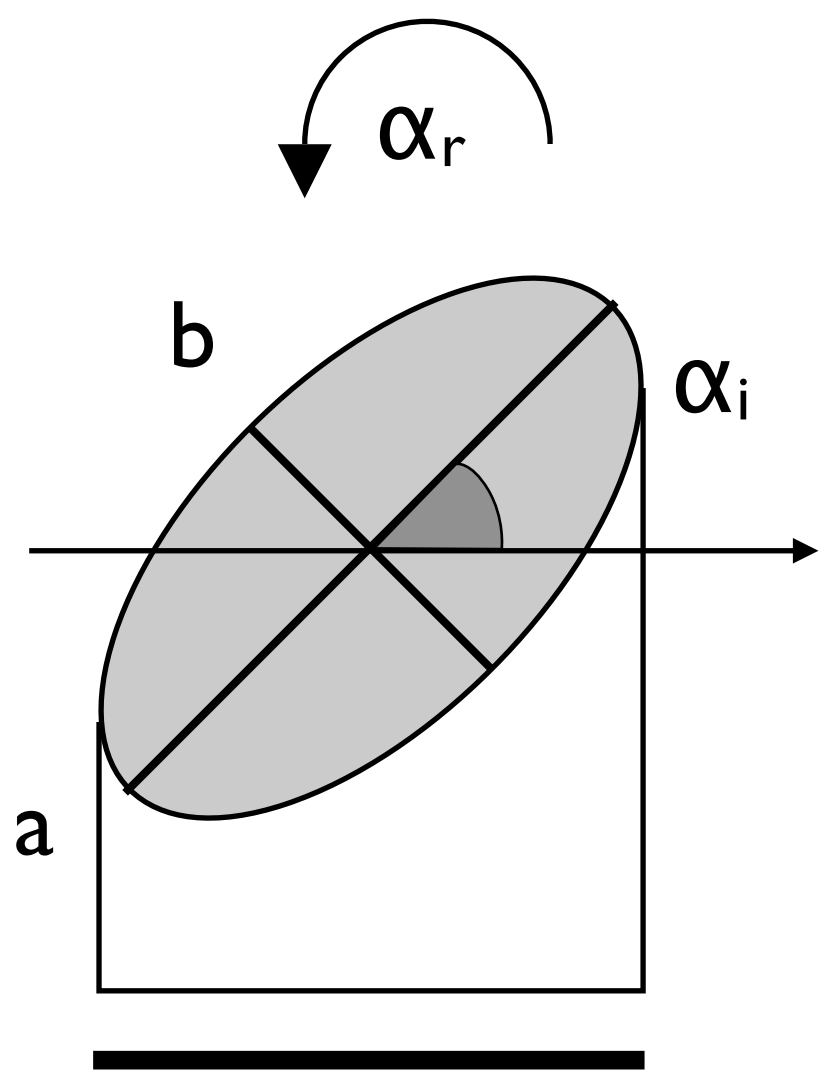


Figure I4.2

Projections of a single ellipse.

The length of projection, P , depends on the orientation, α , of the ellipse with respect to the x-axis and the length of the short and long axes, b and a . Here, the axial ratio, b/a , is 0.5.

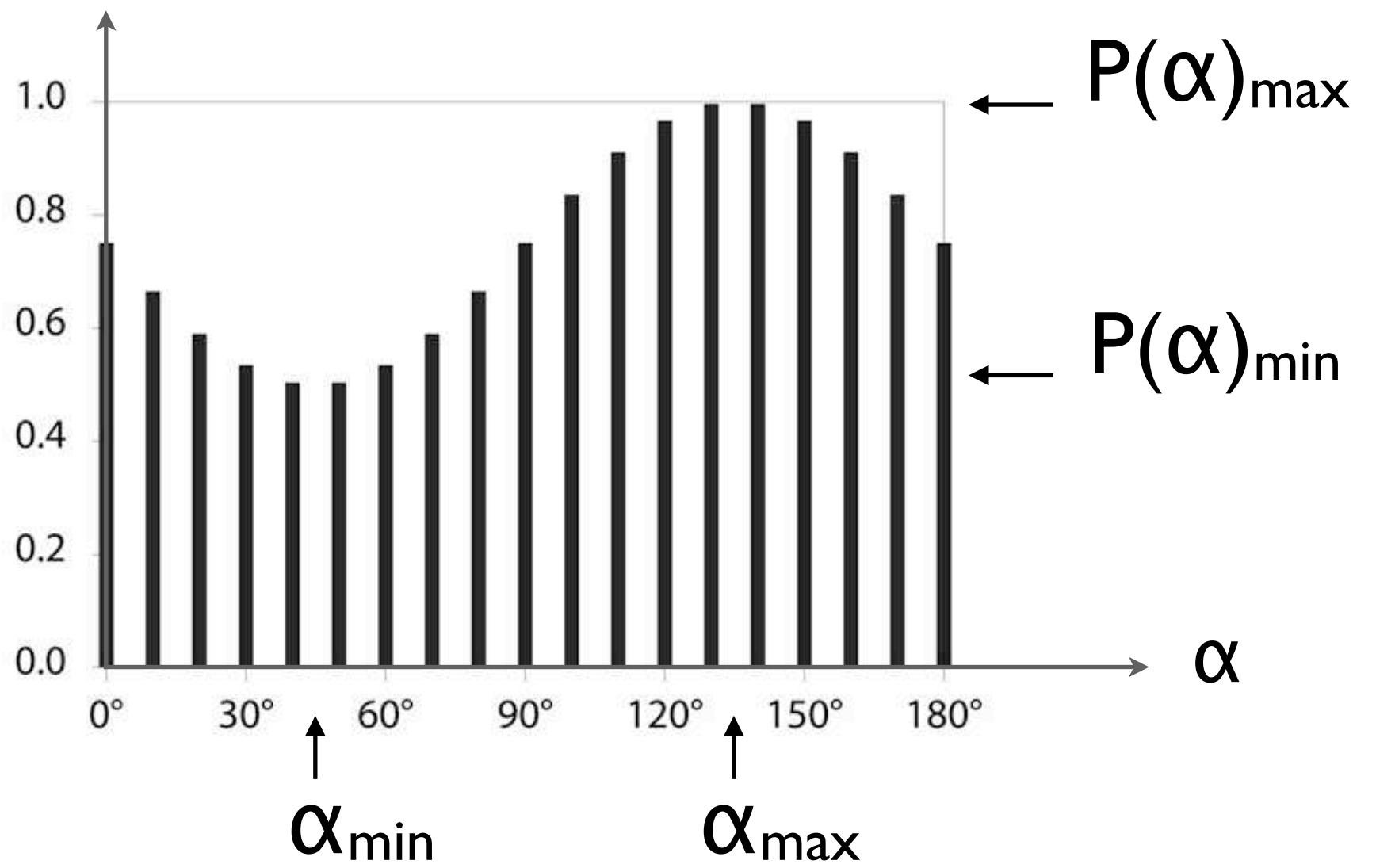


$P(\alpha)$

$\alpha_r = 0^\circ$

$\alpha_i = 45^\circ$

$P(\alpha)$



$$b/a = P(\alpha)_{\min} / P(\alpha)_{\max}$$

$$\alpha_i = 90^\circ - \alpha_{\min} = 180^\circ - \alpha_{\max}$$

Figure 14.3

Projection curve, $P(\alpha)$, of a rotating ellipse.

The length of projection, P , depends on the initial orientation, α_i , of the ellipse and changes as a function of rotation, α_r , ($0^\circ \leq \alpha_r \leq 180^\circ$). The shortest and the longest projections, $P(\alpha)_{\min}$ and $P(\alpha)_{\max}$, occur at angles α_{\min} and α_{\max} , respectively, when either the shortest or the longest axis, b or a , is parallel to the x-axis. Here, the axial ratio, b/a , is 0.5.

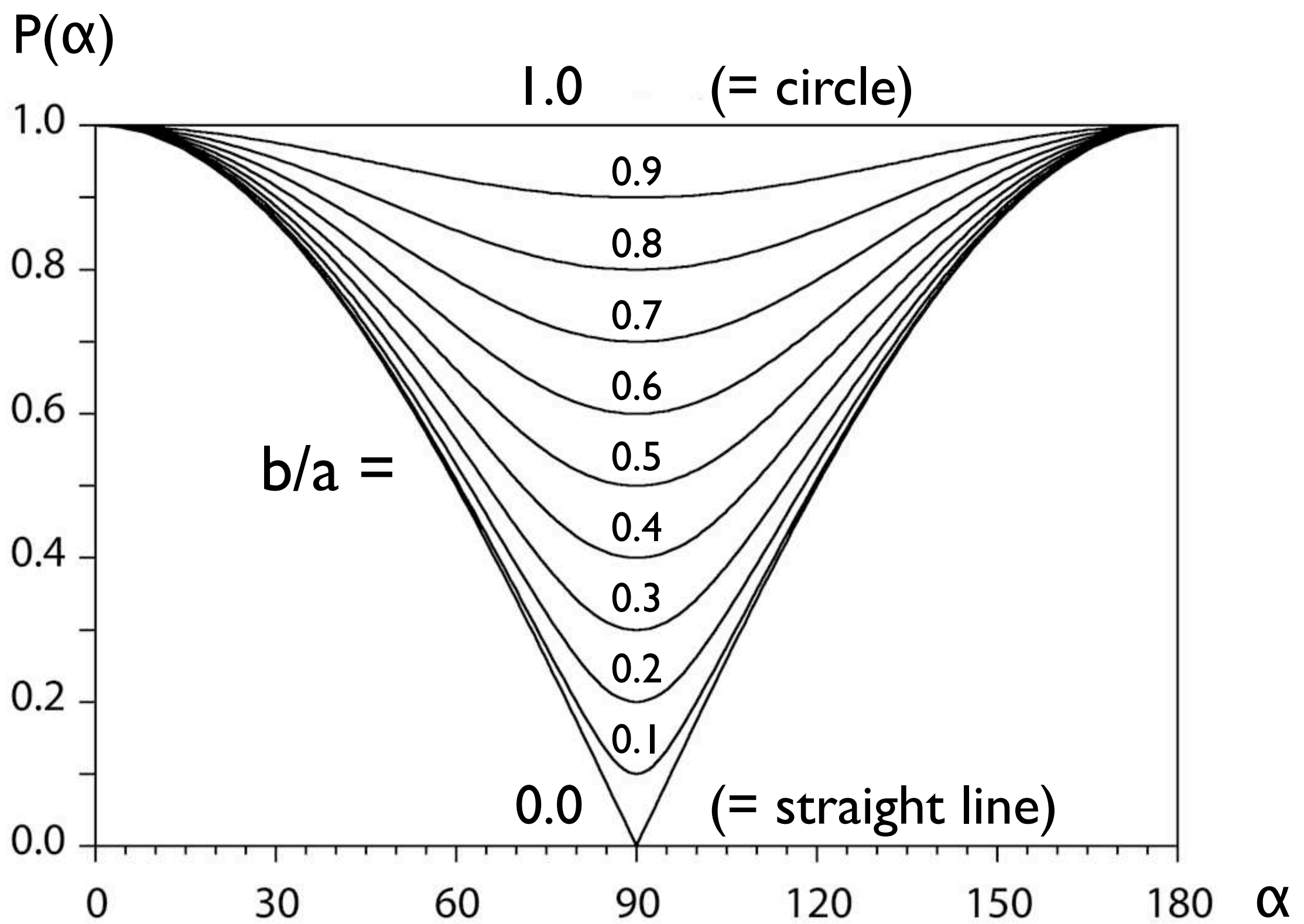


Figure 14.4

Projection curves of rotating ellipses with different axial ratios.

The ellipses are initially parallel to the x-axis, i.e., the initial orientation, $\alpha, = 0^\circ$ and the long diameter, $2a$, is 1.00. The projection curves, $P(\alpha)$, are shown for different axial ratios b/a of the ellipses: if $b/a = 0$, the ellipse is a line, if $b/a = 1.00$, the ellipse is a circle.

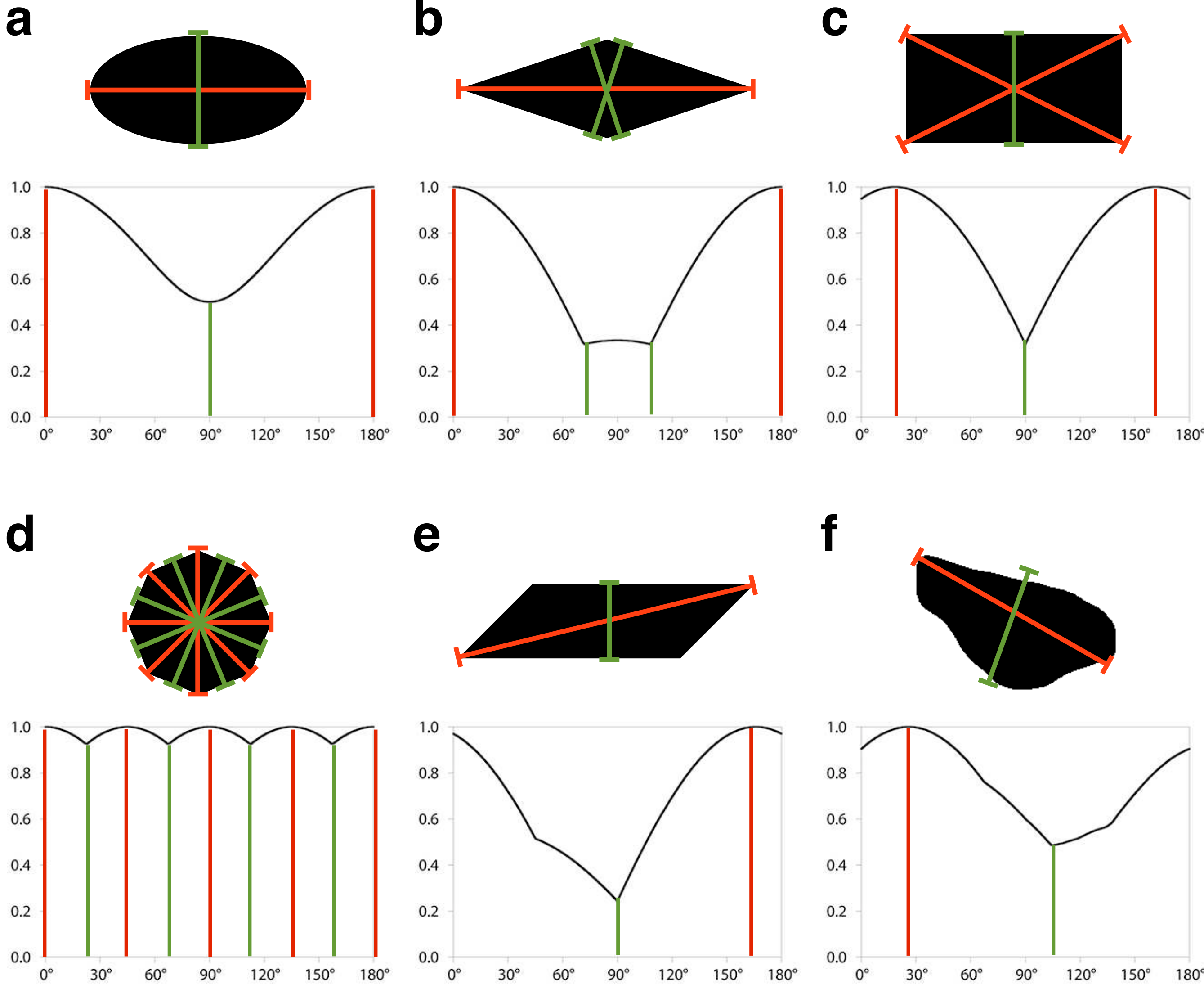


Figure 14.5

Projection functions of elliptical and non-elliptical shapes.
 Longest projections in red - shortest projections in green.

- (a) Ellipse: one minimum, one maximum, minimum and maximum are 90° apart
- (b) rhomb: two minima, one maximum
- (c) rectangle: one minimum, two maxima
- (d) octagon: four minima, four maxima
- (e) oblique quadrangle: one minimum, one maximum, minimum and maximum are not 90° apart
- (f) 'natural' shape: one minimum, one maximum, minimum and maximum are not 90° apart.

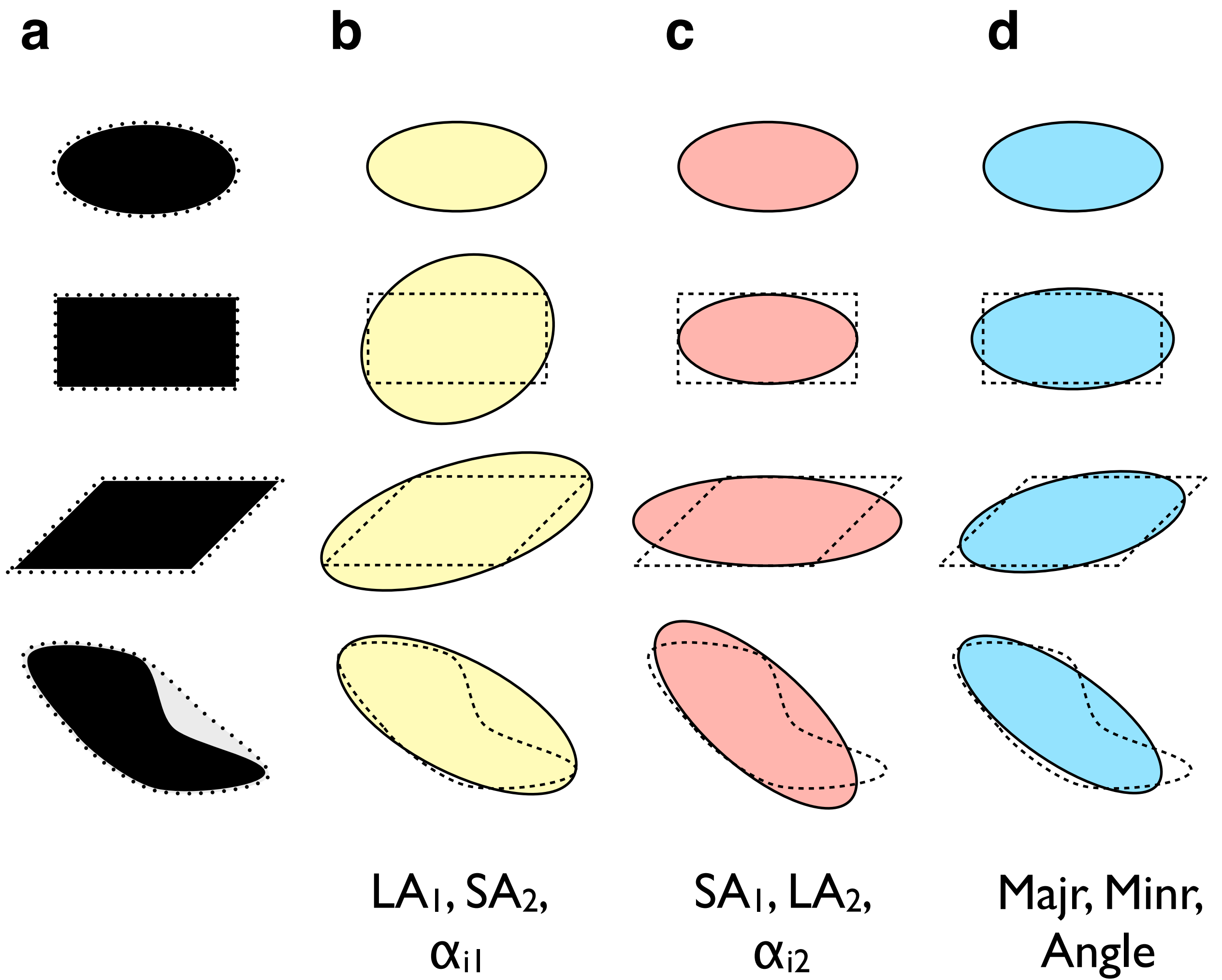


Figure 14.6

Long and short axes of elongate shapes.

(a) Original shapes with convex hull (stippled);

(b - d) best-fit ellipses with original outlines shown as dashed lines;

(b) the long axis, LA_1 , is defined as the longest projection, the short axis, SA_2 , as the projection normal to the longest;

(c) the short axis, SA_1 , is defined as the shortest projection, the long axis, LA_2 , as the projection normal to it;

(b, c) the angles, α_{i1} and α_{i2} , are the orientation of the long axes, LA_1 and LA_2 , respectively, counterclockwise from positive x-axis;

(d) the axes and orientation of the best-fit ellipse are calculated using Image SXM Analyze.

L - ellipse	S - ellipse	SXM - ellipse
$a = LA_1$ $b = SA_2$ $\alpha_{i1} = \text{orientation of } LA_1$	$b = SA_1$ $a = LA_2$ $\alpha_{i2} = \text{orientation of } LA_2$	$a = \text{Majr}$ $b = \text{Minr}$ $\alpha = \text{Angle}$



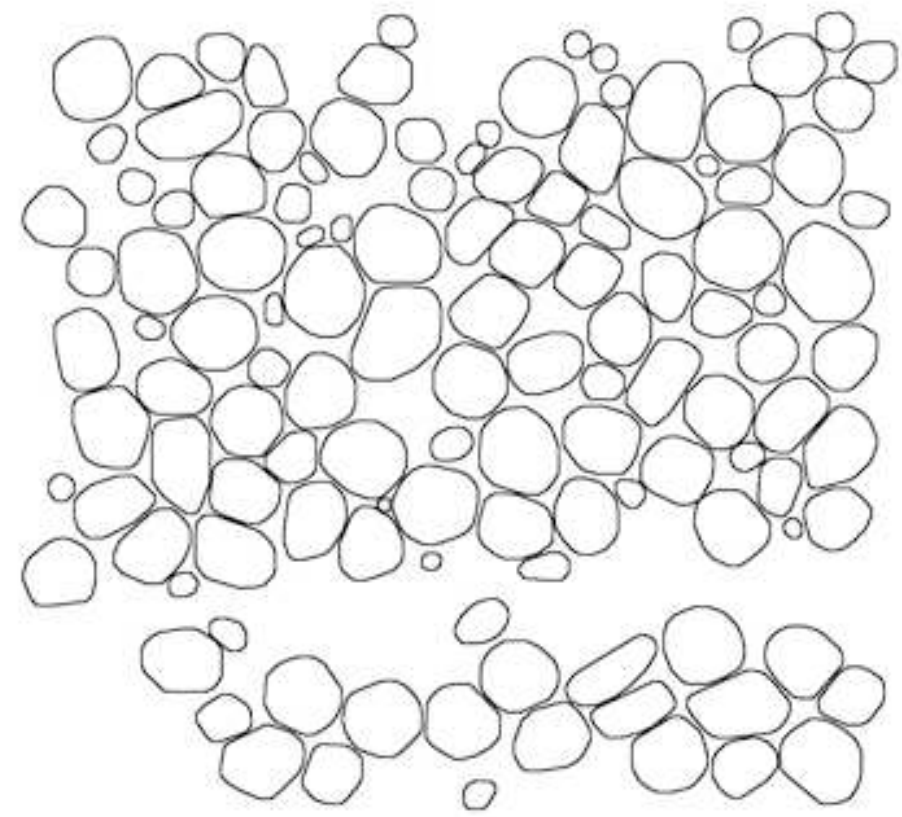
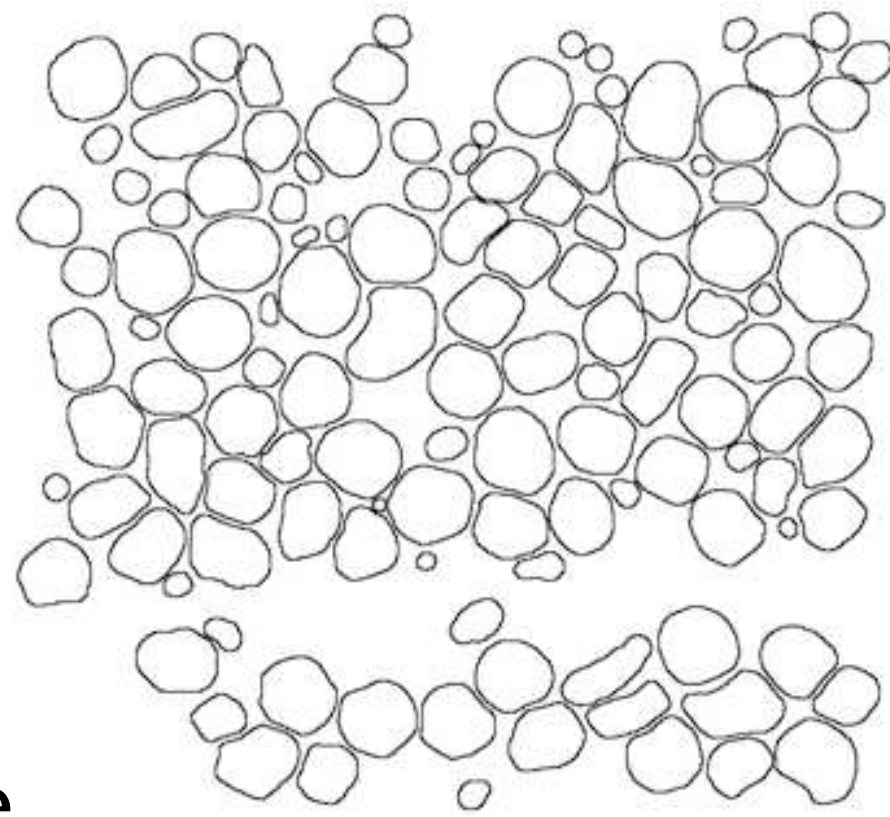
shape	b/a	$\alpha_{i1} (^{\circ})$	b/a	$\alpha_{i2} (^{\circ})$	b/a	$\alpha (^{\circ})$
1 	0.50	0	0.50	0	0.50	0
2 	0.80	153	0.50	0	0.50	0
3 	0.40	162	0.33	0	0.38	167
4 	0.42	28	0.40	42	0.38	35

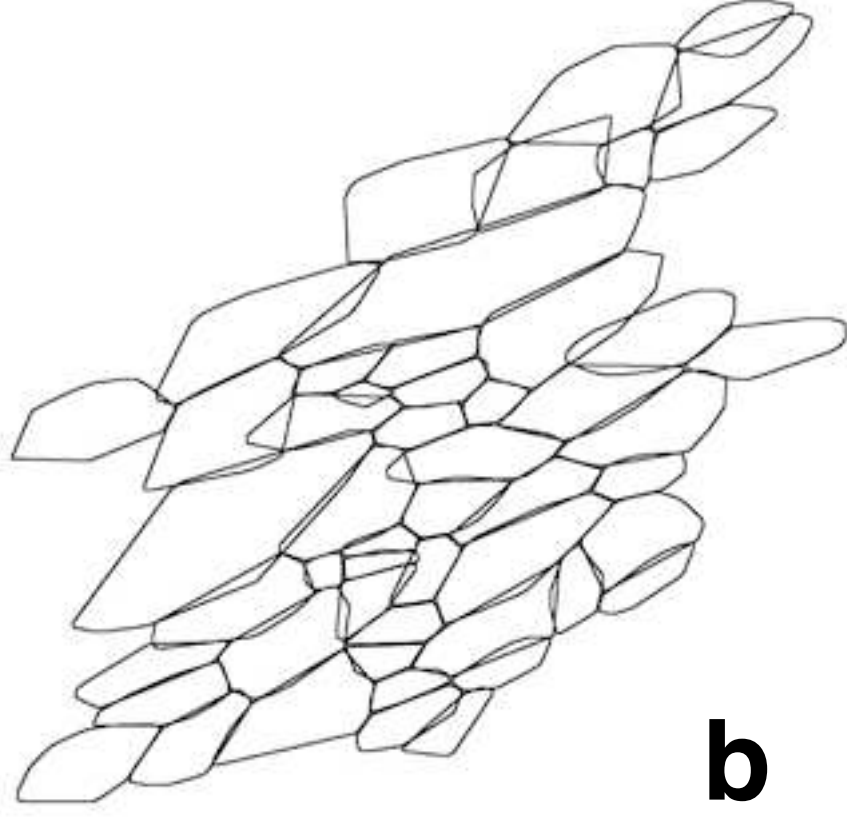
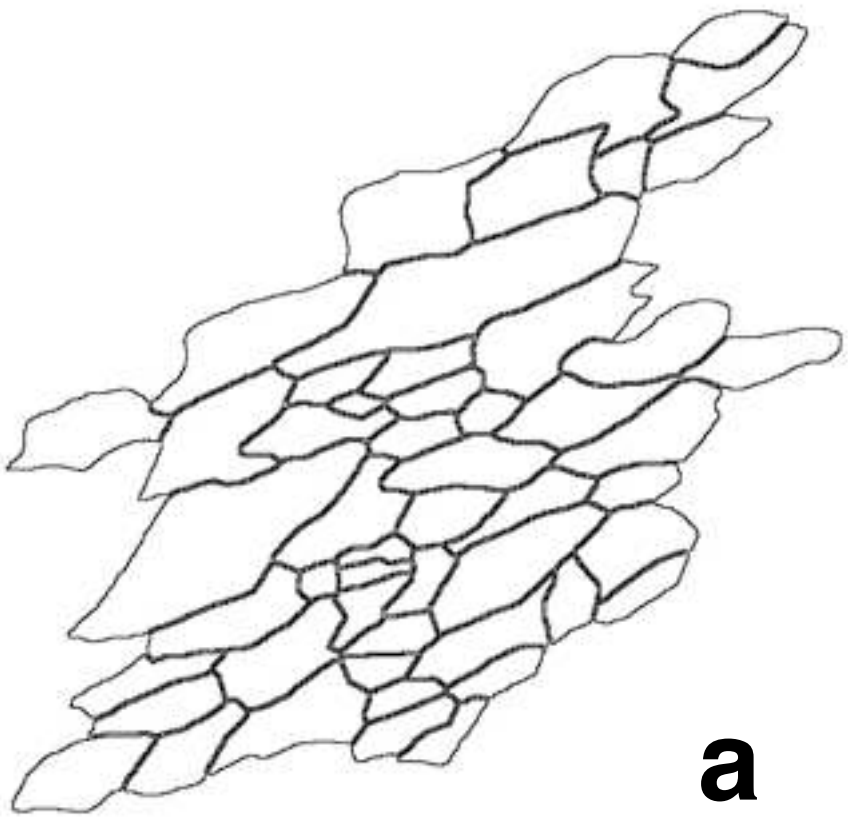
Table I4.1

Best-fit ellipses.

For definition of LA_1 , LA_2 , SA_1 , SA_2 , α_{i1} , α_{i2} , see Figure I4.6; for definition of Majr, Minr and Angle, see Figure 8.2. Shapes are the same as in Figure I4.6; b/a = axial ratio; b = short axis; a = long axis; α_{i1} , α_{i2} , α = orientation of long axis, angles CCW from positive x-axis.



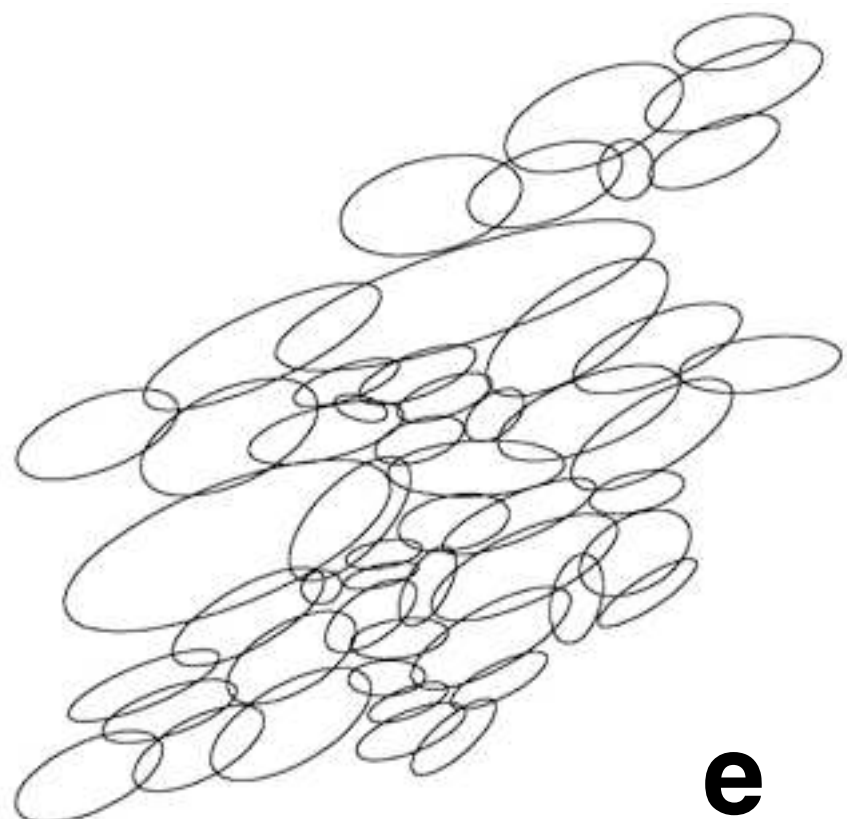
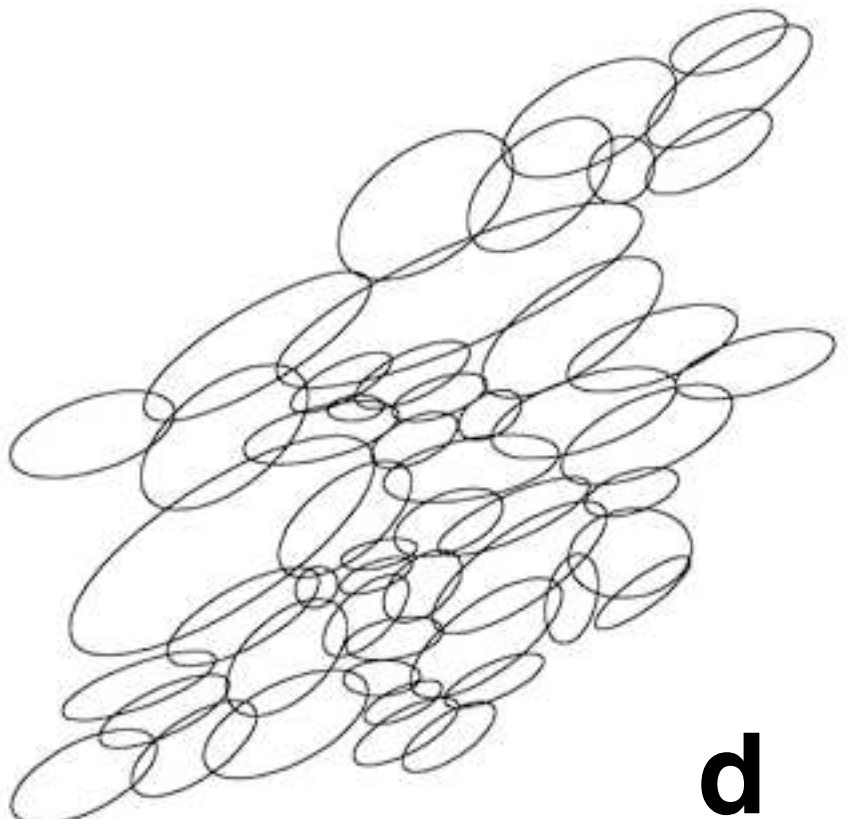
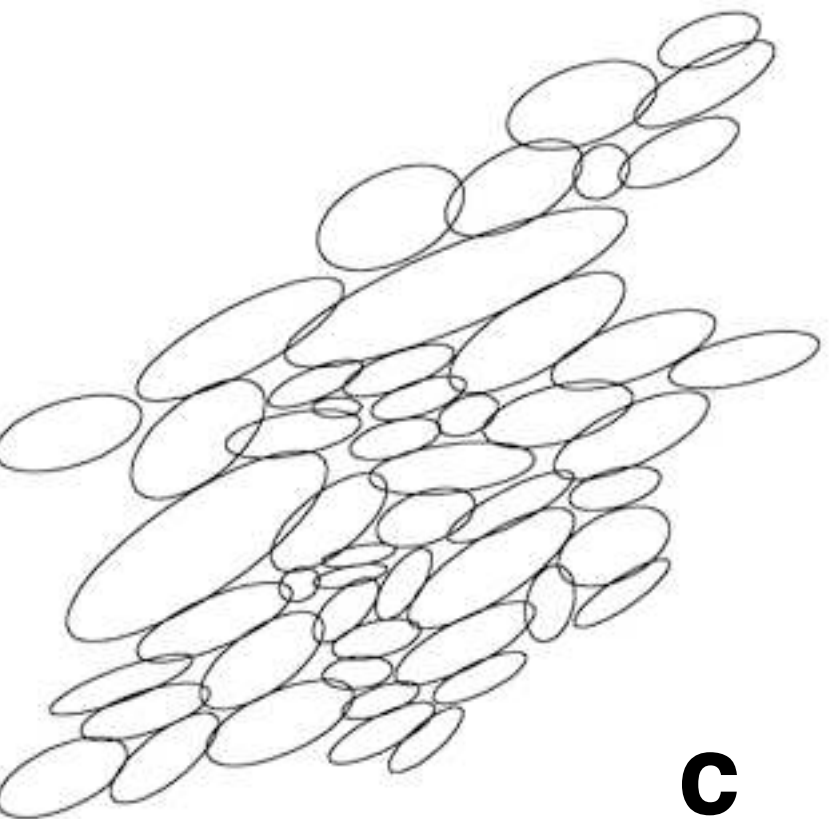
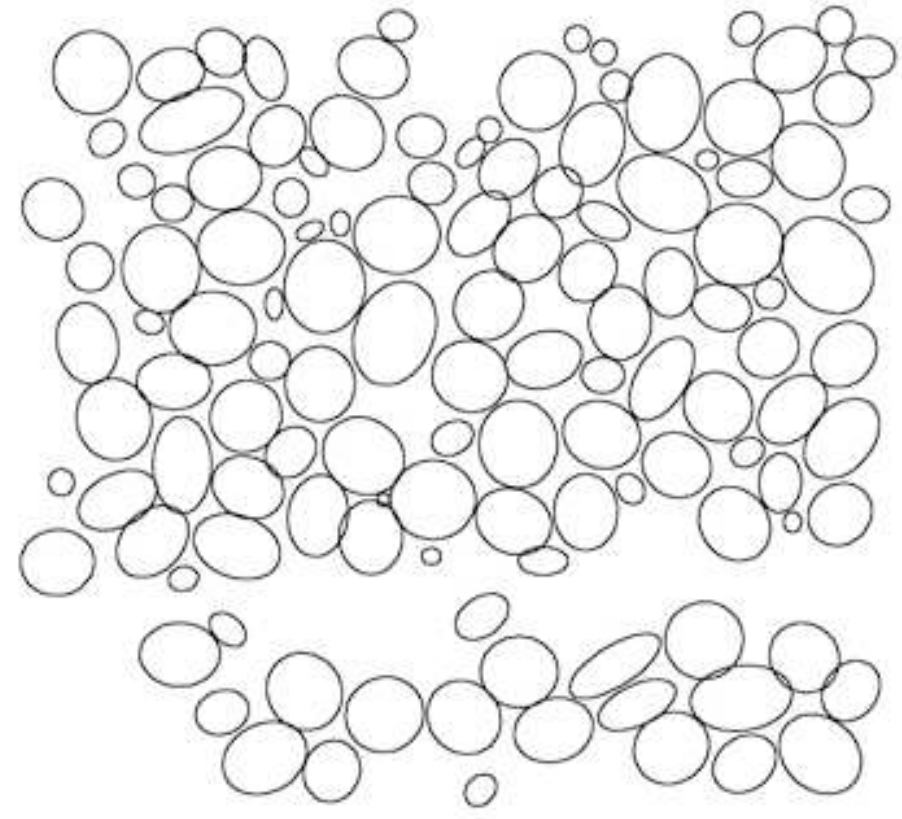
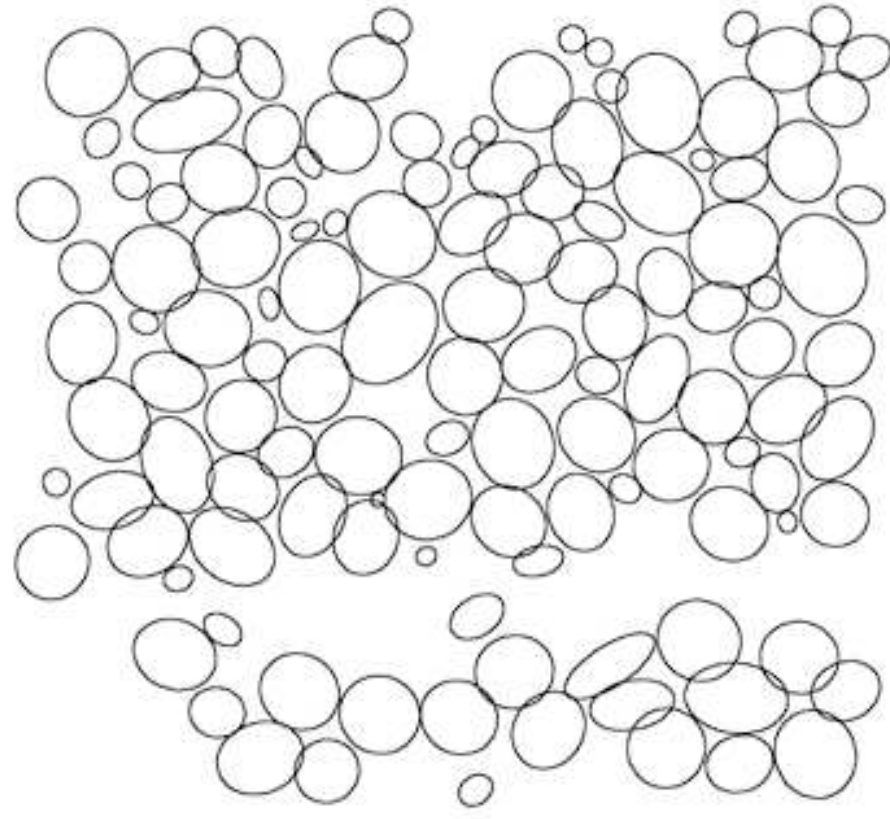
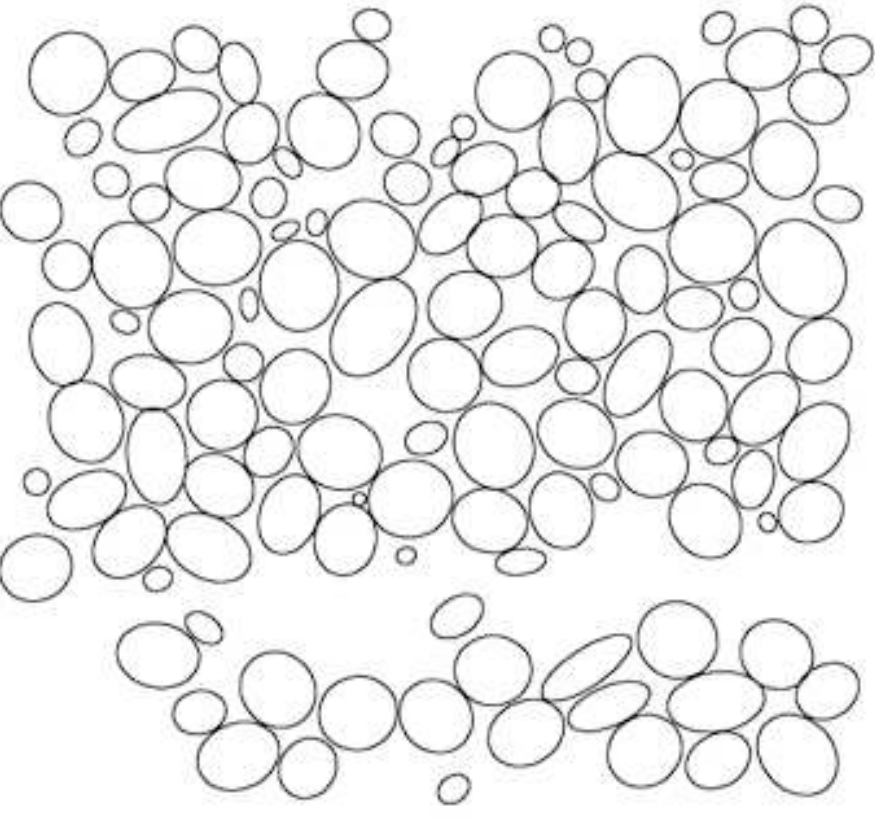
oolithic limestone



sheared marble

a

b



c

d

e

Figure 14.7

Outlines, convex hulls and best-fit ellipse approximations.

(a) Original fabric; top: particle in matrix = oolitic limestone (Hauptrogenstein, Jura Mountains Switzerland); bottom: crystalline aggregate = experimentally sheared Carrara marble (600°C, $\gamma = 1.22$, twinning regime, dextral shear sense);

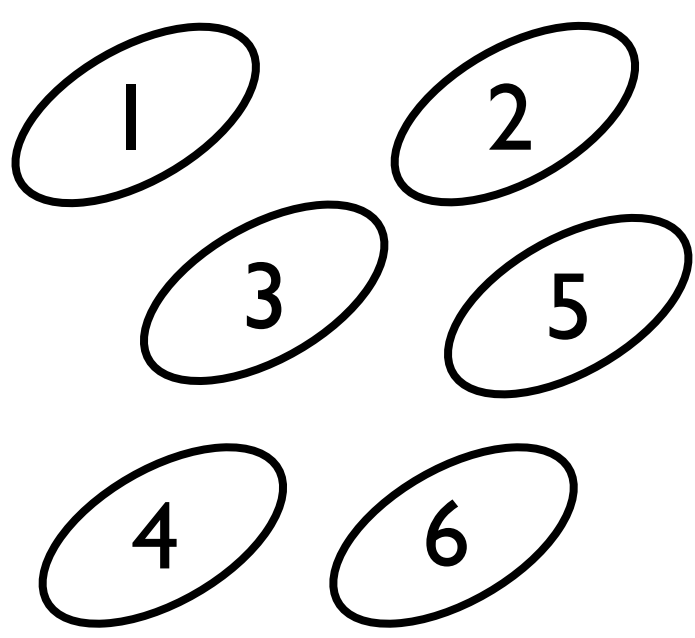
(b) convex hull of the particles;

(c) the axes and orientations of the best-fit ellipses are calculated using Image SXM Analyze.

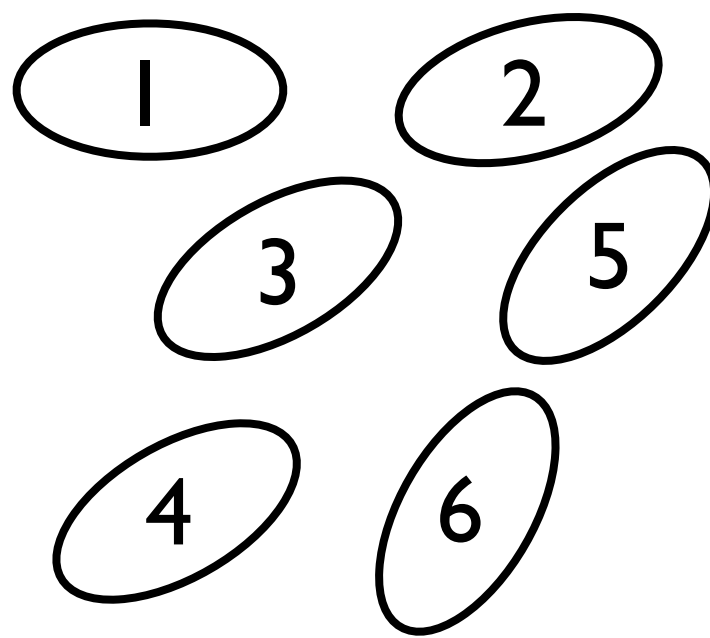
(d) the long axes of the best-fit ellipses, LA_1 , are defined as the longest, the short axes, SA_2 , as the projections normal to the longest, the angles, α_{i1} are the orientations of the long axes, LA_1 ;

(e) the short axes of the best-fit ellipses, SA_1 , are defined as the longest, the long axes, LA_2 , as the projections normal to the shortest, the angles, α_{i2} are the orientations of the long axes, LA_2 .

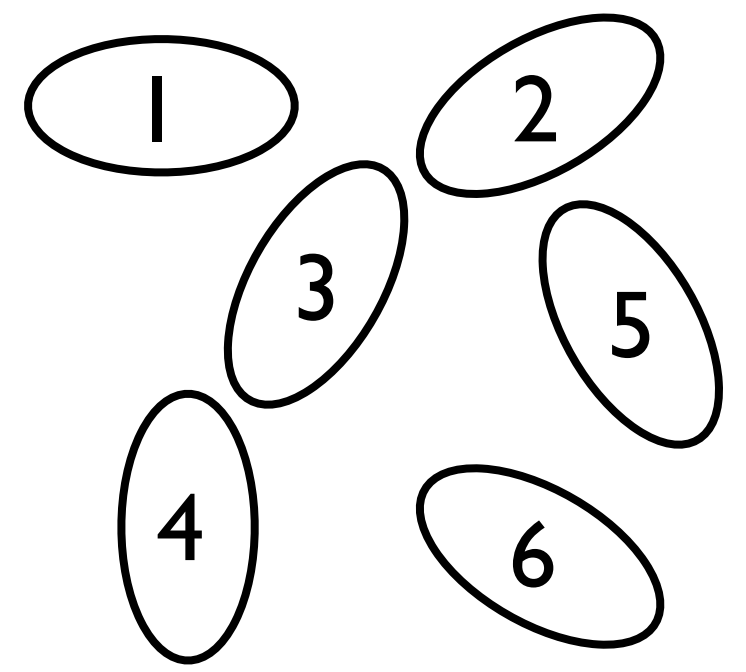
For better comparison with (c), the ellipses in (d) and (e) are also scaled to the size of the particles.



parallel



aligned



random

$B(\alpha)$

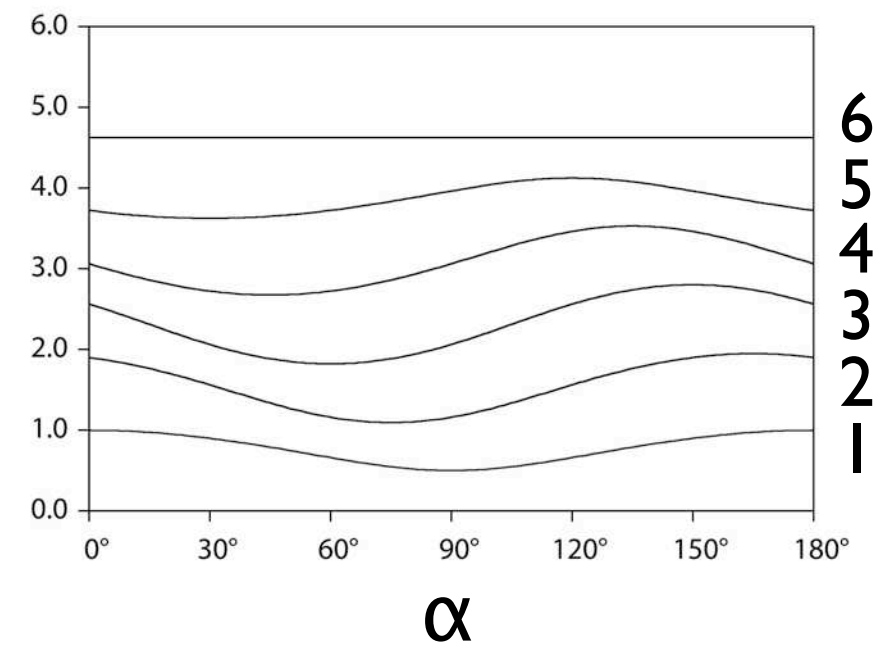
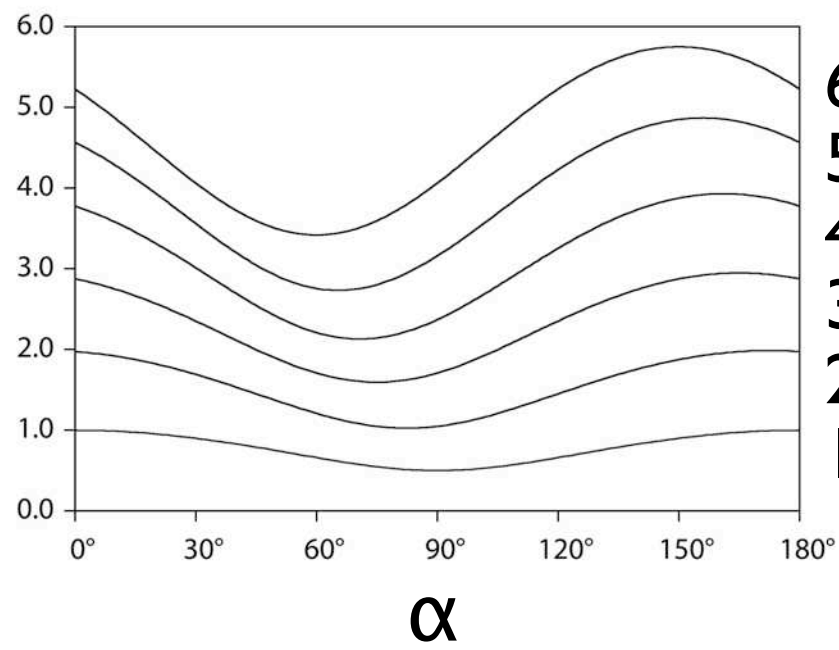
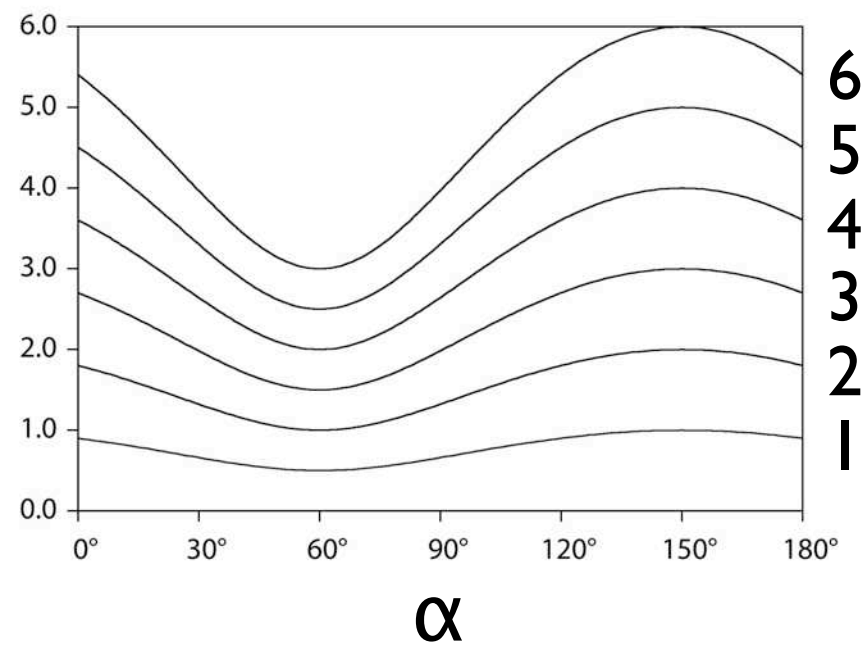


Figure 14.8

Projection curves, $B(\alpha)$, of sets of ellipses.

The projection curves of the individual ellipses (labeled 1 to 6) are shown as cumulative plots.

(a) Parallel ellipses: orientation distribution function (ODF) = delta function: $h(\alpha_i) = \infty$ if $\alpha_i = 30^\circ$; fabric as a whole has same anisotropy as individual ellipses

(b) ellipses with preferred orientation: ODF = normal distribution: $h(\alpha_i) = 30^\circ \pm 10^\circ$; fabric as a whole is less anisotropic than individual ellipses

(c) randomly oriented ellipses: ODF = uniform distribution; fabric as a whole is isotropic.

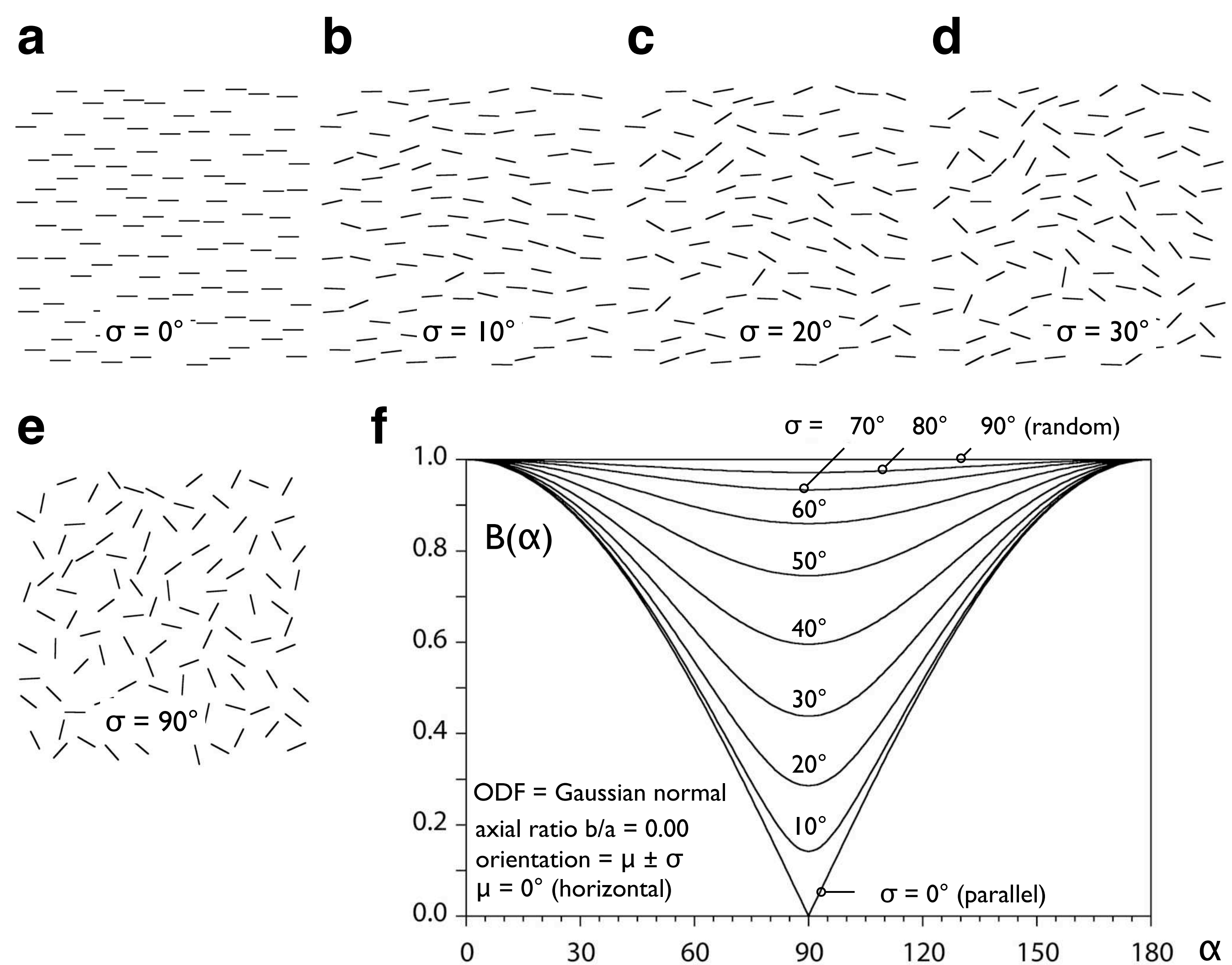


Figure 14.9

Line fabrics and projection curves $B(\alpha)$.

Orientation of lines is described in terms of normal distributions with mean orientation, $\mu = 0^\circ$ and different standard deviations.

(a) Perfectly parallel lines: $h(\alpha_i) = 1.00$; or normal distribution with $\mu = 0^\circ$; $\sigma = 0^\circ$;

(b - d) preferred orientation of lines: $h(\alpha_i) =$ normal distribution with $\mu = 0^\circ$; $\sigma = 10^\circ, 20^\circ$ and 30° ;

(e) random orientation of lines: $h(\alpha_i) = 1.00$; or normal distribution with $\mu = 0^\circ$; $\sigma = 90^\circ$;

(f) projection curve $B(\alpha)$ of sets of 100 lines; $B(\alpha)$ is normalized such that $B(\alpha)_{\max} = 1.00$.

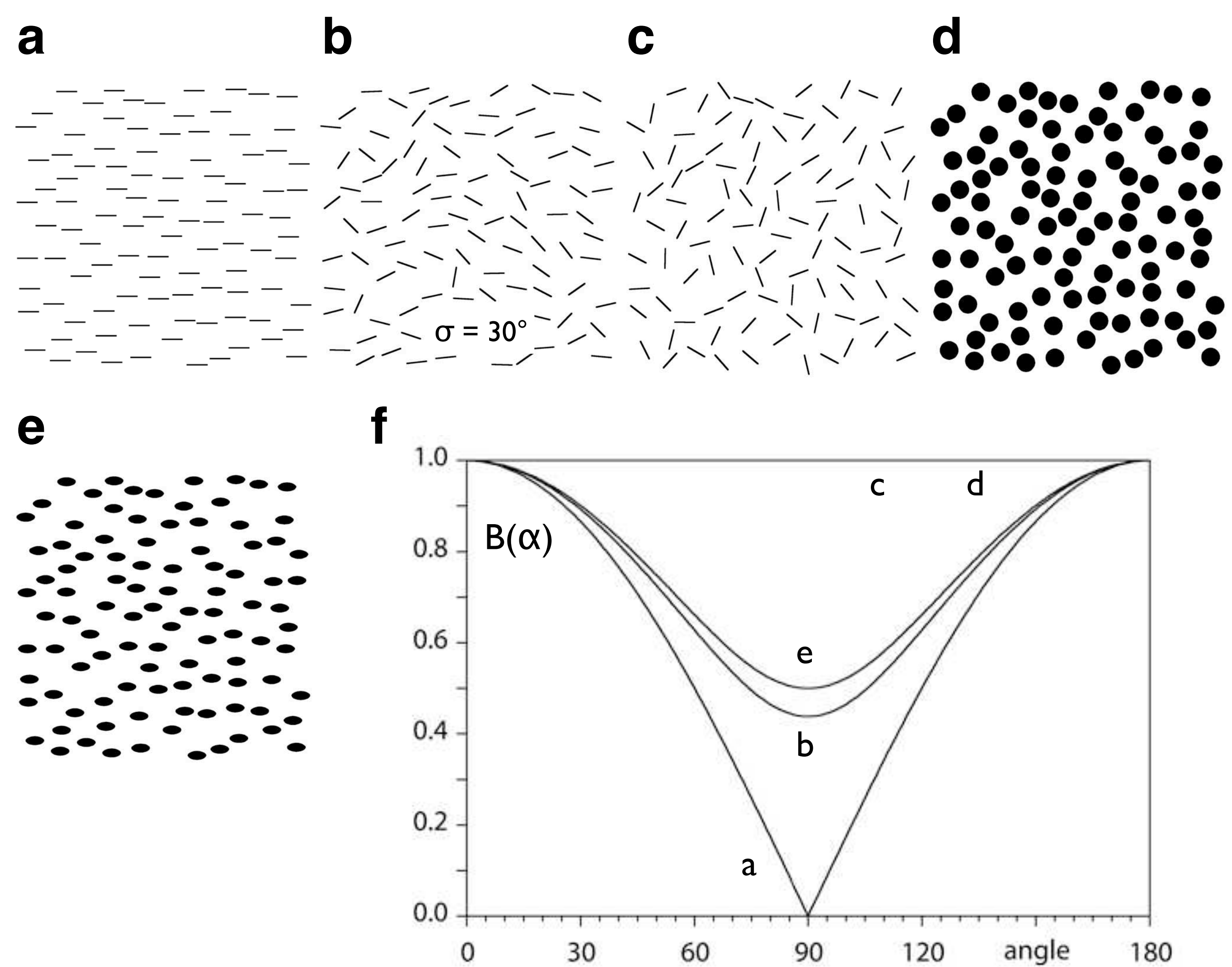


Figure 14.10

Effect of increasingly random orientation and increasing axial ratio on bulk fabric.

(a) Perfectly parallel lines: $b/a = 0.00$; $h(\alpha_i) = \text{delta function}$;

(b) preferred orientation of lines: $b/a = 0.00$; $h(\alpha_i) = \text{normal distribution}$;

(c) random orientation of lines: $b/a = 0.00$; $h(\alpha_i) = \text{uniform distribution}$;

(d) circles: $b/a = 1.0$;

(e) perfectly parallel ellipses: $b/a = 0.5$; $h(\alpha_i) = \text{delta function}$;

(f) projection curves of fabrics (a - e); $B(\alpha)$ is normalized such that $B(\alpha)_{\max} = 1.00$.

gs172 x-y coordinates smoothed

16662

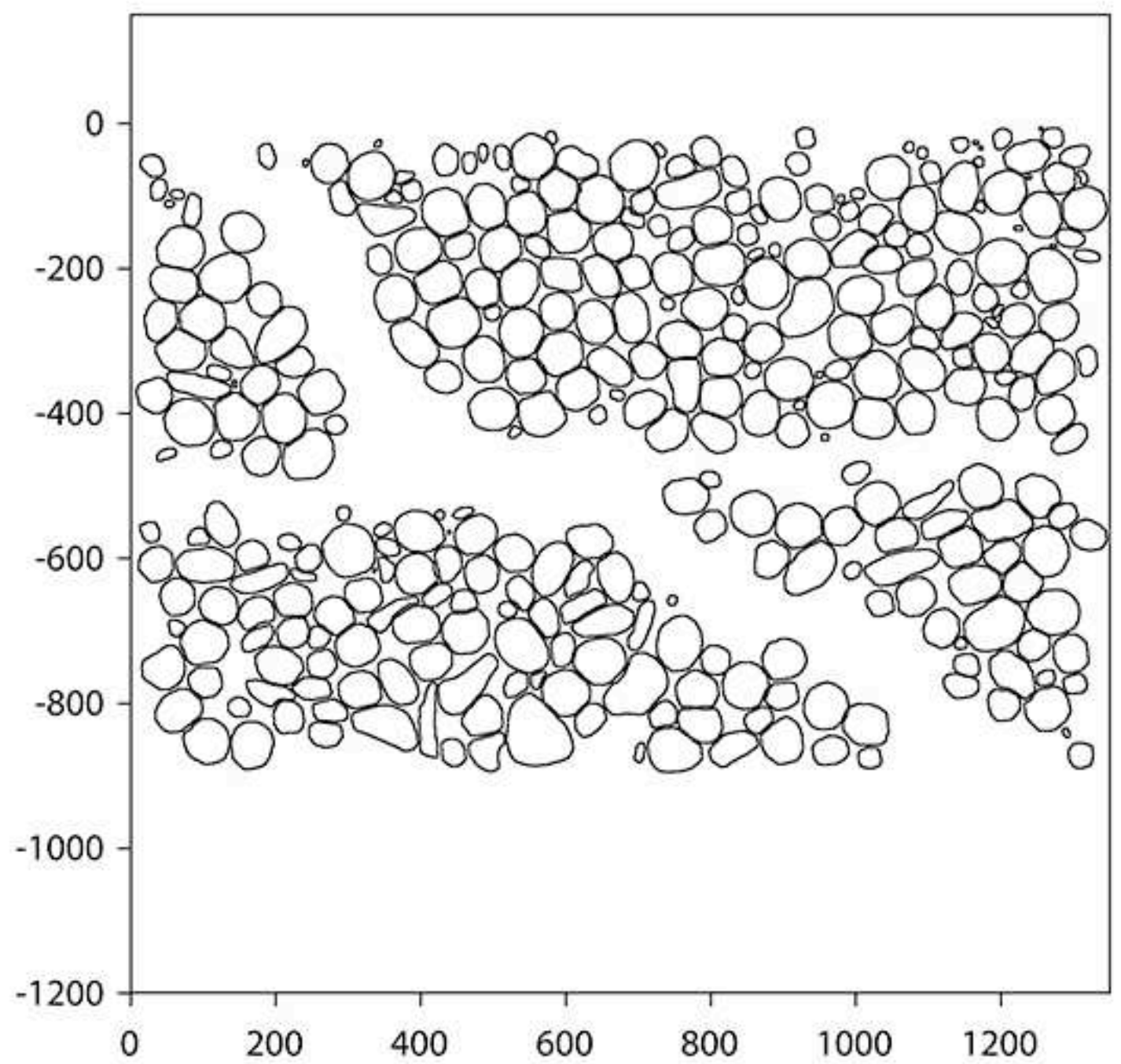
927.24701	-5.5961385
928.28491	-5.6106129
933.92932	-6.1165819
936.13708	-6.8479538
938.95685	-8.0975637
939.92847	-8.9699326

.... etc.

926.55768	-5.8526130
927.24701	-5.5961385
9999.0000	9999.0000

.... etc.

1009.1608	-863.35156
1010.9039	-862.68860
1013.5924	-861.67352
1014.4003	-861.39825
9999.0000	9999.0000



Software Box 14.1

Input file gs172.cor.scm with x-y coordinates of particle outlines; plot of file.

*** paror ***

2010-11-24, rh

analysis of bulk particle fabric
maximum number of points per particles is 1000
maximum number of particles is 5000

input file:

line 1:	bti(132byte)	title (must have)
line 2:	n	total number of points
for each particle:	x,y	floating x-y coordinates
etc.
	Xend,Yend	end coordinates

name of file >

1

gs172.cor.scm

end coordinate of input file (0, 9999, ... one number):

2

9999

increment of rotation angle (minimum: 1 deg.) >

3

10

do you want printout (0), file (1), both (2) ? >

4

1

5

name of output file ? [gs172.cor.p10] (return=default) >

6

name of file with B(alfa) curve ? [gs172.cor.j10] >

7

name of file with long-axes ODF ? [gs172.cor.x10] >

8

name of file with particle data ? [gs172.cor.d10] >

Software Box 14.2

Dialog with program PAROR; answers are numbered and highlighted, see text for explanation.

10°	5°	1°	file type
file.p10	file.p05	file.p01	screen output
file.d10	file.d05	file.d01	axes and orientations
file.j10	file.j05	file.j01	B(α) curve
file.x10	file.x05	file.x01	ODF of long axes

Table 14.2

Default file name extensions used for result files created by the PAROR program. For angular resolutions of 10° , 5° and 1° .

paror analysis of gs172.cor.scm

1

```

B(alfa)min =          44.762          B(alfa)max =          47.549
Alfamin =          75.          Alfamax =          14.
Bulk b/a =          0.94138

```

```

Angular difference =          119.
(diff < 90 deg = dextral monoclinic)

```

```

Preferred orientation (of LA1) alfap1 = 166.
Preferred orientation (of LA2) alfap2 = 15.

```

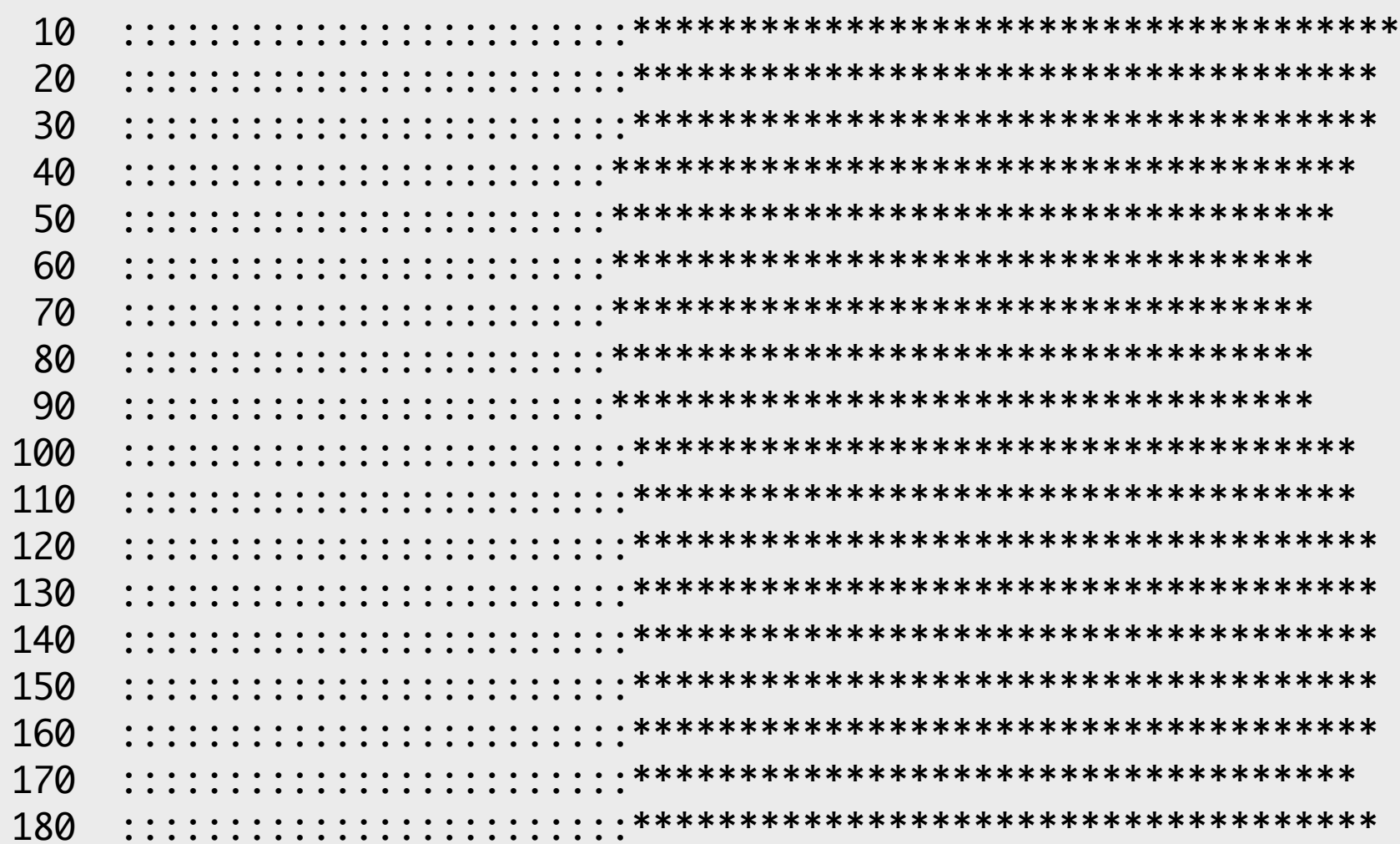
2

length of projections, B(alpha), (= Feret diam.)

angle	mean	variance	st.dev.	skewness
10	47.51385	384.32730	19.60427	-0.23660
20	47.45034	376.00531	19.39086	-0.24753
30	46.98285	361.55994	19.01473	-0.24991
40	46.32403	351.31671	18.74344	-0.23435
50	45.60604	341.57437	18.48173	-0.21703
60	45.08461	335.89786	18.32752	-0.20634
70	44.79977	335.37720	18.31331	-0.19058
80	44.77297	338.23099	18.39106	-0.17372
90	45.08445	350.80429	18.72977	-0.19561
100	46.10207	362.16537	19.03064	-0.19748
110	46.60590	367.72769	19.17623	-0.19149
120	46.86028	366.88049	19.15413	-0.18453
130	47.05245	369.35434	19.21859	-0.18661
140	47.23512	372.40295	19.29774	-0.18645
150	47.32745	376.34705	19.39967	-0.17898
160	47.15906	379.88049	19.49052	-0.16303
170	46.72064	378.98520	19.46754	-0.15489
180	46.88687	387.06946	19.67408	-0.20411

3

histogram: average length of projection versus angle of projection



Software Box I4.3
 PAROR output file gs172.cor.p10:

(1) Calculation of $B(\alpha)_{max}$, $B(\alpha)_{min}$, α_{max} and α_{min} using an evaluation at 1° increments, angular difference is between α_{max} and α_{min} ;

(2) Length of projection, $B(\alpha)$, list of values;

(3) Mean length of projection and standard deviation, shown as histogram;

evaluation of particle axes:

	number of projected particles: 343	mean	variance	st.dev.	skewness
longest projection		51.8276	430.4483	20.7472	-0.1907
shortest projection		39.6860	279.0329	16.7043	-0.2845
perp. to longest		41.4572	298.4258	17.2750	-0.3207
perp. to shortest		50.6558	426.2610	20.6461	-0.1372
perp.L/longest		0.8053	0.0207	0.1440	-1.1211
shortest/longest		0.7680	0.0183	0.1352	-1.0944
shortest/perp.S		0.7905	0.0212	0.1456	-1.0217
perp.L/perp.S		0.8294	0.0249	0.1578	-0.9547

4

5

histogram of long axes and number of long axes LA1 versus angle of rotation

average length of long axes:

number of long axes:

55.47	10	*****	6	10	****
43.88	20	*****	16	20	*****
52.72	30	*****	26	30	*****
52.30	40	*****	23	40	*****
58.02	50	*****	18	50	*****
43.69	60	*****	20	60	*****
53.99	70	*****	28	70	*****
57.62	80	*****	15	80	*****
60.43	90	*****	13	90	*****
43.48	100	*****	13	100	*****
39.46	110	*****	14	110	*****
41.96	120	*****	11	120	*****
55.32	130	*****	14	130	*****
54.32	140	*****	24	140	*****
48.31	150	*****	21	150	*****
51.23	160	*****	41	160	*****
58.36	170	*****	32	170	*****
56.10	180	*****	8	180	*****

histogram of long axes and number of long axes LA2 versus angle of rotation

6

average length of long axes:

number of long axes:

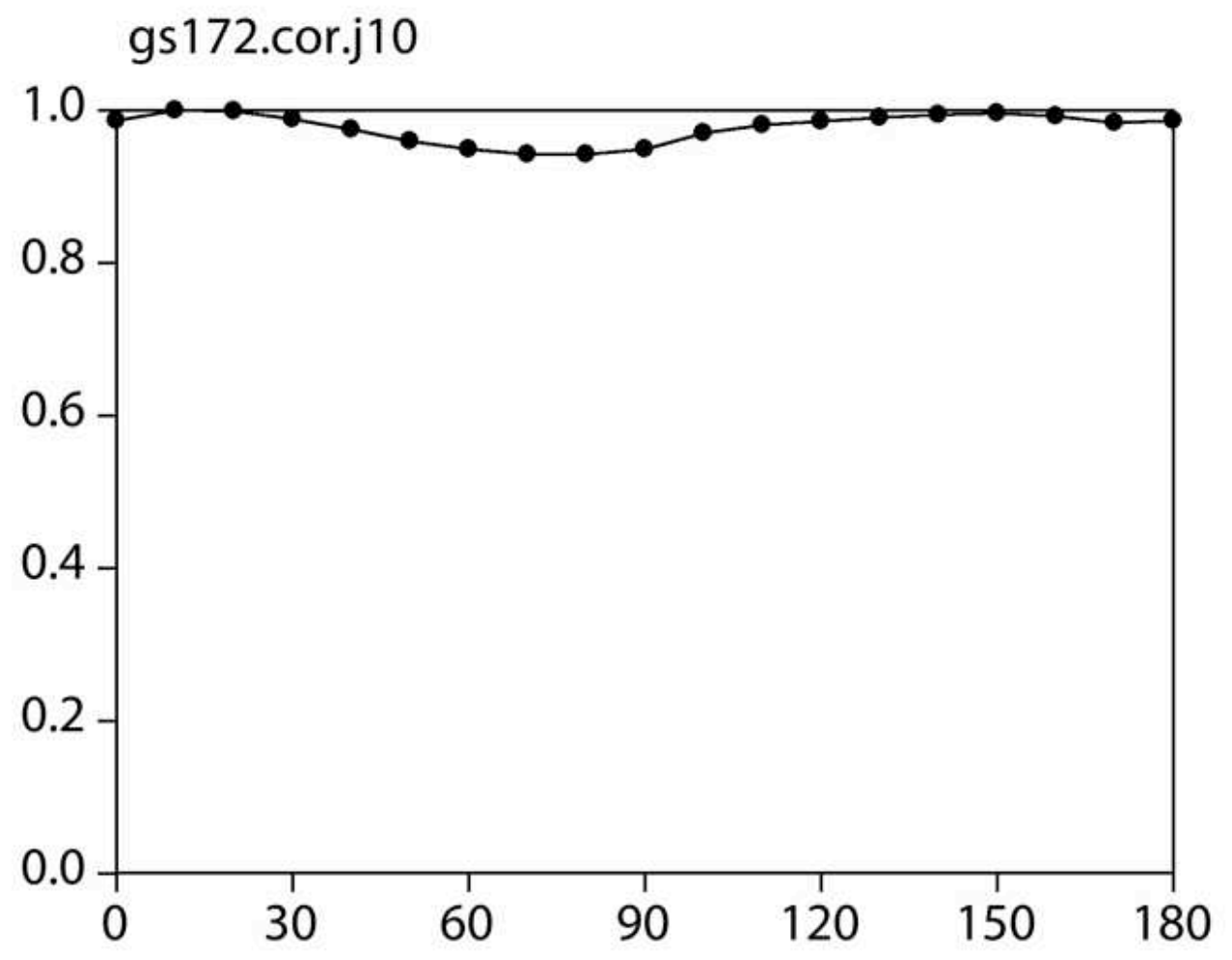
54.29	10	*****	33	10	*****
49.71	20	*****	28	20	*****
59.64	30	*****	27	30	*****
53.75	40	*****	27	40	*****
56.98	50	*****	16	50	*****
62.63	60	*****	8	60	*****
58.97	70	*****	8	70	*****
51.08	80	*****	7	80	*****
34.83	90	*****	31	90	*****
50.66	100	*****	28	100	*****
50.02	110	*****	16	110	*****
43.84	120	*****	10	120	*****
62.69	130	*****	11	130	*****
58.40	140	*****	10	140	*****
56.56	150	*****	13	150	*****
47.53	160	*****	15	160	*****
56.79	170	*****	13	170	*****
40.26	180	*****	42	180	*****

Software Box I4.3

PAROR output file gsI72.cor.pI0:

- (4) Axes and axial ratios of particles;
- (5) Length and number of long axes LA₁ versus orientation;
- (6) Length and number of long axes LA₂ versus orientation.

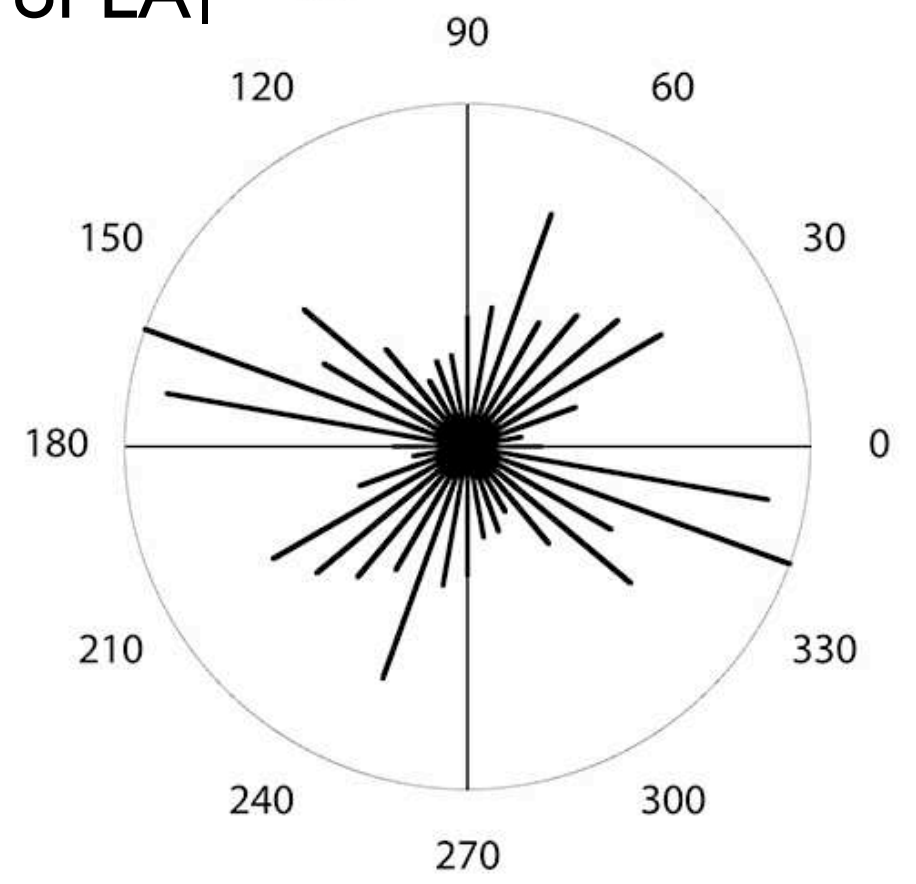
angle	rel_length_of_proj
0	0.98680
10	1.00000
20	0.99866
30	0.98882
40	0.97496
50	0.95985
60	0.94887
70	0.94288
80	0.94231
90	0.94887
100	0.97029
110	0.98089
120	0.98624
130	0.99029
140	0.99413
150	0.99608
160	0.99253
170	0.98331
180	0.98680



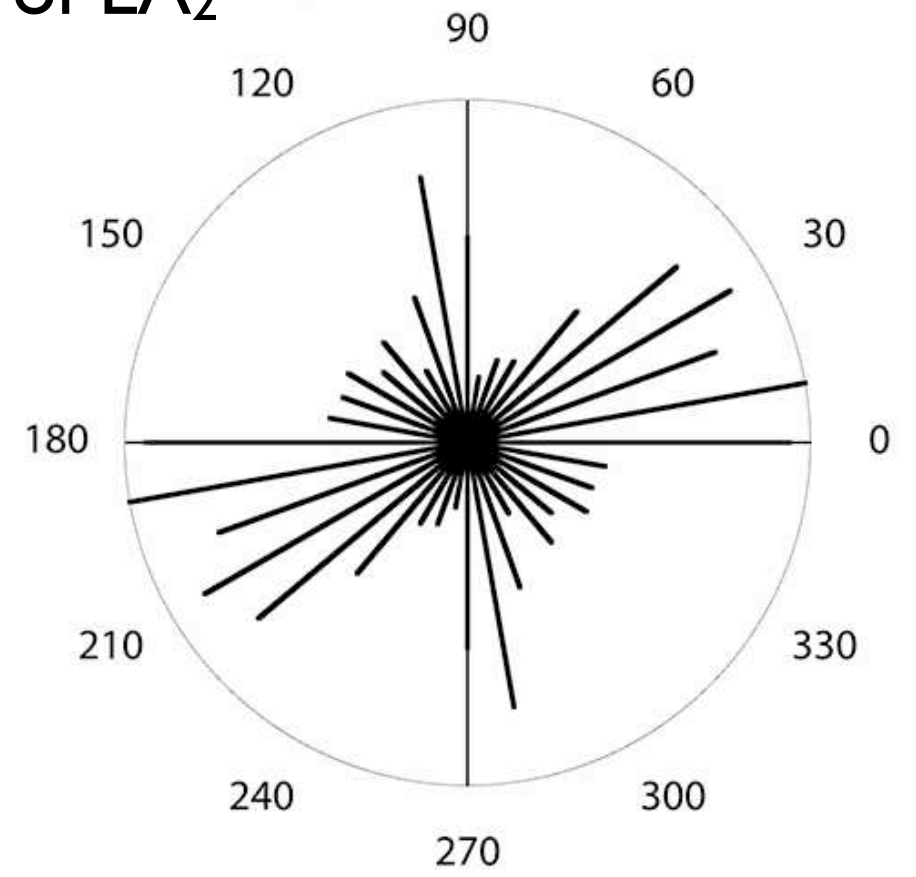
Software Box I4.4

PAROR output file gs172.cor.j10: Values of $B(\alpha)$ and plot.

ODF of LA₁ ^{x10}



ODF of LA₂ ^{g10}



angle	rel_length_LA1	rel_length_LA2
-180.0	0.21367	0.94366
-175.0	0.00000	0.00000
-170.0	0.15845	1.00000
-165.0	0.00000	0.00000
-160.0	0.33429	0.77693
-155.0	0.00000	0.00000
-150.0	0.65264	0.89880
-145.0	0.00000	0.00000
-140.0	0.57269	0.80994

..... etc.

135.0	0.00000	0.00000
140.0	0.62068	0.32597
145.0	0.00000	0.00000
150.0	0.48298	0.41040
155.0	0.00000	0.00000
160.0	1.00000	0.39790
165.0	0.00000	0.00000
170.0	0.88910	0.41206
175.0	0.00000	0.00000
180.0	0.21367	0.94366

Software Box I4.5

PAROR output file gs172.cor.x10: Length weighted orientation distributions (ODF) of long axes, LA₁ and LA₂, and rose diagrams. Intermediate zero values (at 5°, 15°, etc.) are inserted to facilitate plotting of the rose diagrams.

paror analysis of gs172.cor.scm

number of particles: 343

minimum number of points/particle : 3

maximum number of points/particle : 1000

increment of rotation : 10

#	longest(LA1)	shortest(SA1)	perp.L(SA2)	perp.S(LA2)	SA2/LA1	SA1/LA1	alfaLA1	alfaLA2	mkl	Xc	Yc
1	29.5026	24.8078	29.2895	28.2858	0.9928	0.8409	140.	100.	40.	930.24	-18.73
2	4.6351	3.7804	3.8694	3.7931	0.8348	0.8156	40.	0.	40.	1254.75	-7.01
3	31.1801	27.5646	28.0435	29.8744	0.8994	0.8840	150.	0.	-30.	1269.88	-20.06
4	29.9597	24.5553	25.2841	29.8036	0.8439	0.8196	60.	50.	10.	1202.01	-20.69
5	18.5911	13.4676	13.7404	18.2917	0.7391	0.7244	110.	120.	-10.	580.51	-20.60
6	63.9011	59.7227	60.3972	62.8714	0.9452	0.9346	100.	40.	60.	555.33	-43.85
7	46.6194	38.0730	38.2518	44.6852	0.8205	0.8167	130.	110.	20.	792.63	-36.75
8	24.3700	20.7269	21.7226	23.7549	0.8914	0.8505	170.	0.	-10.	1145.09	-29.18
9	13.1649	8.9011	8.9036	13.0755	0.6763	0.6761	50.	40.	10.	340.97	-26.89
10	72.8184	66.3386	68.1621	69.0571	0.9361	0.9110	70.	30.	40.	694.44	-56.23
11	8.5161	5.7747	5.9877	7.7660	0.7031	0.6781	160.	0.	-20.	1164.60	-25.83
12	63.8346	43.2561	46.0511	63.4958	0.7214	0.6776	0.	10.	-10.	1236.91	-45.41
13	16.1638	13.7806	14.8526	14.7670	0.9189	0.8526	60.	90.	-30.	1072.67	-31.97
14	22.4911	12.9760	14.0573	22.3257	0.6250	0.5769	110.	120.	-10.	729.91	-35.82
15	34.8403	22.8076	22.8076	34.8403	0.6546	0.6546	100.	100.	0.	187.99	-45.67
16	56.1935	50.1285	52.2959	54.6604	0.9306	0.8921	70.	50.	20.	275.06	-53.77
17	44.3838	34.9235	35.6008	44.0069	0.8021	0.7869	80.	90.	-10.	434.05	-48.03
18	25.7133	13.6912	13.7793	25.5773	0.5359	0.5325	90.	100.	-10.	486.00	-40.85
19	35.8567	21.2694	22.9016	35.0314	0.6387	0.5932	110.	100.	10.	511.97	-46.75
20	42.9562	29.2222	31.3816	42.0580	0.7305	0.6803	30.	10.	20.	1303.04	-45.06
21	60.2673	38.3636	40.1192	60.0673	0.6657	0.6366	160.	150.	10.	614.09	-53.61
22	6.0305	4.7959	5.3902	5.7143	0.8938	0.7953	140.	90.	50.	1172.68	-33.68
23	17.2685	14.7920	16.5276	16.7043	0.9571	0.8566	110.	90.	20.	1091.26	-41.03
24	69.8852	64.0367	65.3091	67.8792	0.9345	0.9163	60.	40.	20.	331.27	-71.11
25	29.8251	20.4206	22.2847	28.2261	0.7472	0.6847	70.	100.	-30.	467.30	-53.31

.... etc.

Software Box 14.6

PAROR output file gs172.cor.d10: Axes, axial ratios and orientations of particles:

= number of analyzed particle;

longest (LA1) = longest projection, shortest (SA1) = shortest projection of particle;

perp.(SA2) = projection perpendicular to longest, perp.(LA2) = projection perpendicular to shortest projection of particle;

SA2/LA1 = axial ratio (= short / long axis) based on LA1 = longest projection;

SA1/LA1 = minimum possible value for axial ratio;

alfaLA1 = orientation of longest projection;

alfaLA2 = orientation of normal to shortest projection;

mkl = angular difference between the orientations of LA₁ and LA₂;

X_c and Y_c = center point coordinates of particles calculated as the average x- and the average y-coordinate of the points digitized on the outline.

Angles are CCLW from positive x-axis.

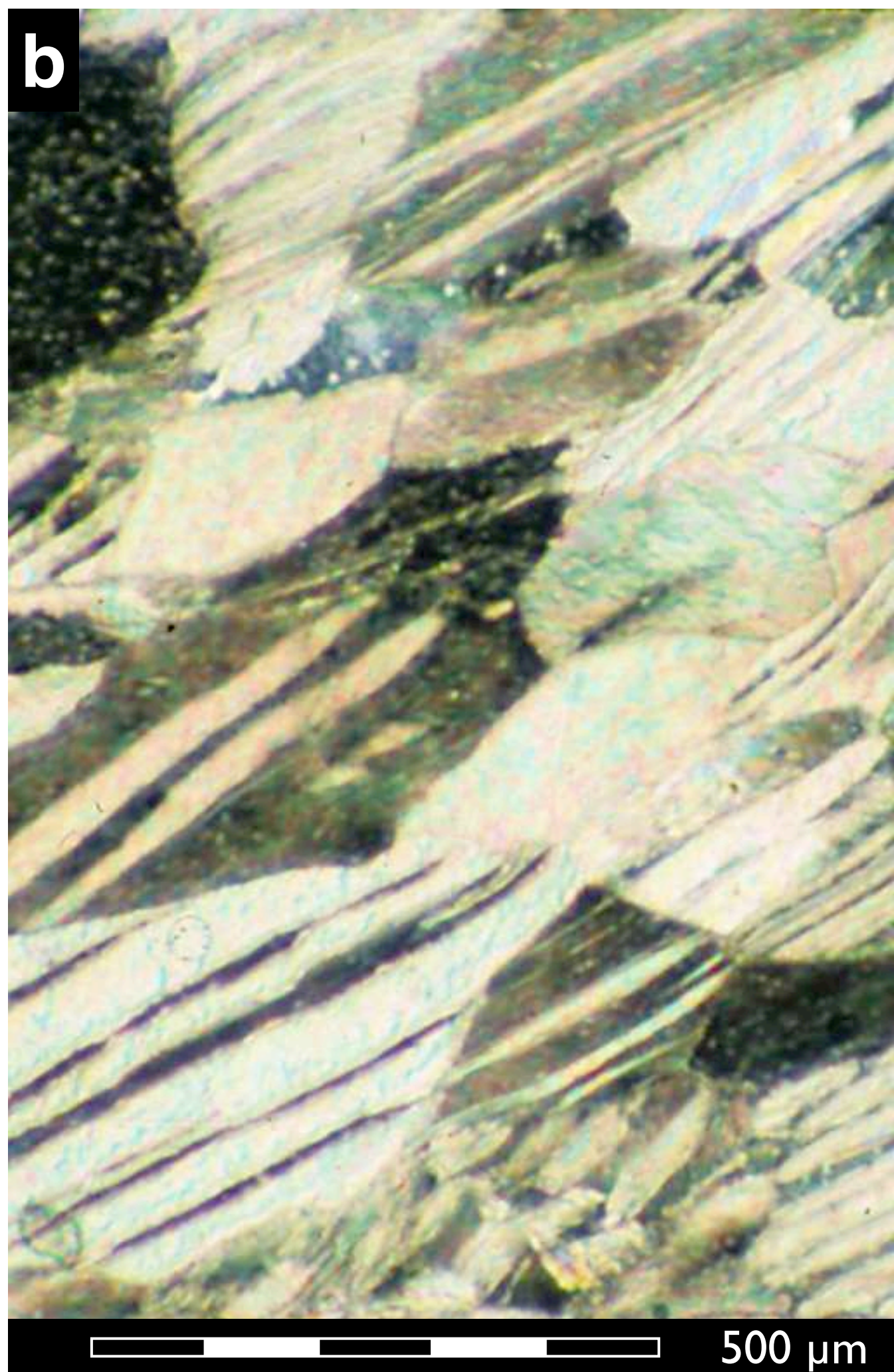
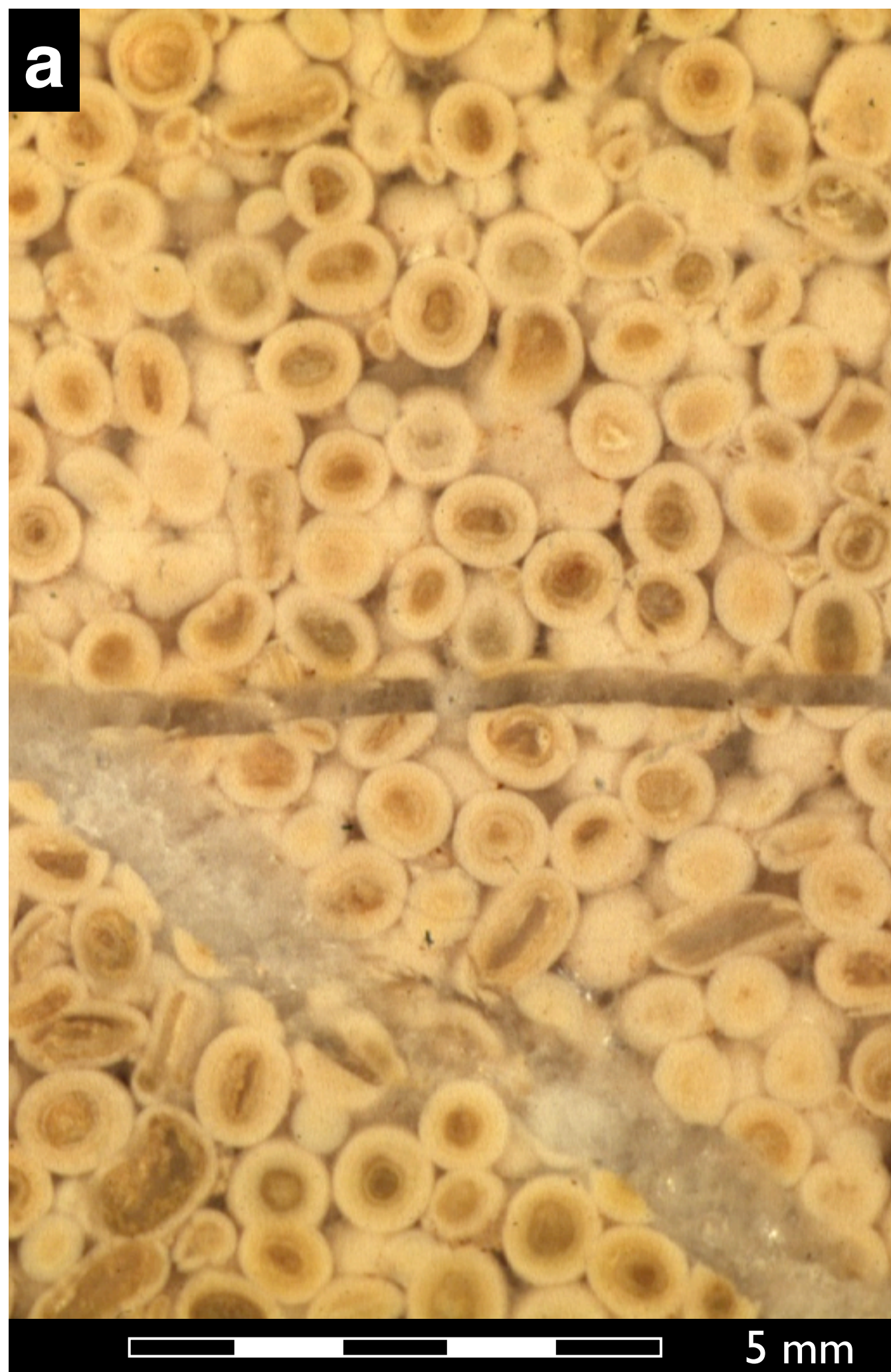


Figure 14.11

Natural examples for particle fabric analysis.

(a) Oolitic limestone of the Hauptrogenstein formation, Jura Mountains, polished surface;

(b) experimentally deformed Carrara marble, thin section, polarized light, sample CTI 600°, intracrystalline slip regime, $\gamma = 1.22$.

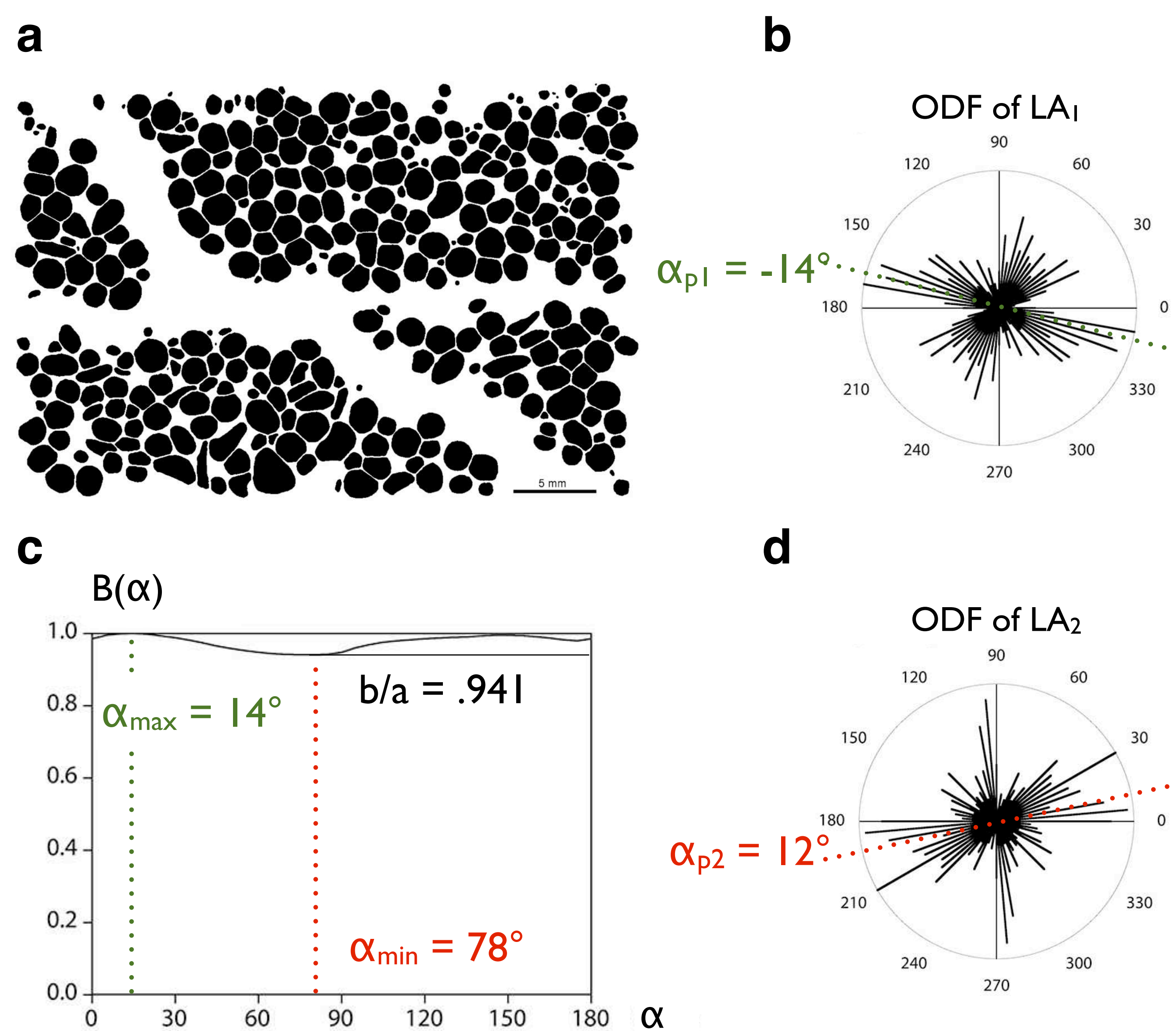


Figure 14.12

PAROR analysis of an oolitic limestone.

(a) Bitmap of fabric (prepared from acetate peel of GS 172);

(b) projection curve B(α) of gs172.cor.scm;

(c) rose diagrams of long axes of particles (5° resolution) using LA₁ axes(longest projections of particles);

(d) same as (c) using LA₂ axes (= projections normal to the shortest projection).

The bulk preferred orientations, α_{p1} (green) and α_{p2} (red), calculated from α_{\max} and α_{\min} , respectively, are superposed on the rose diagrams. (The exact values for b/a , α_{p1} and α_{p2} were derived from analyses made with 1° increment of rotation).

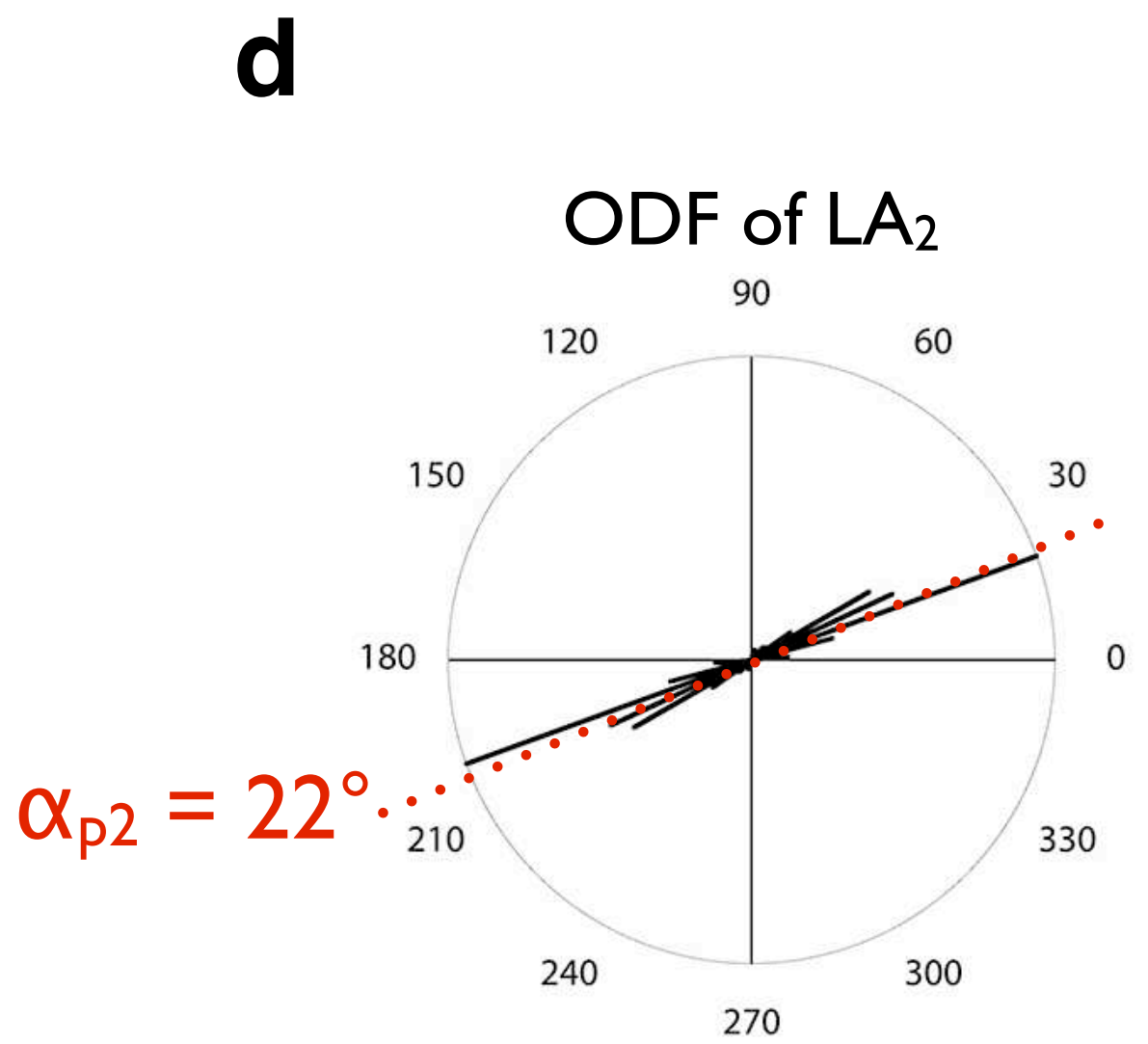
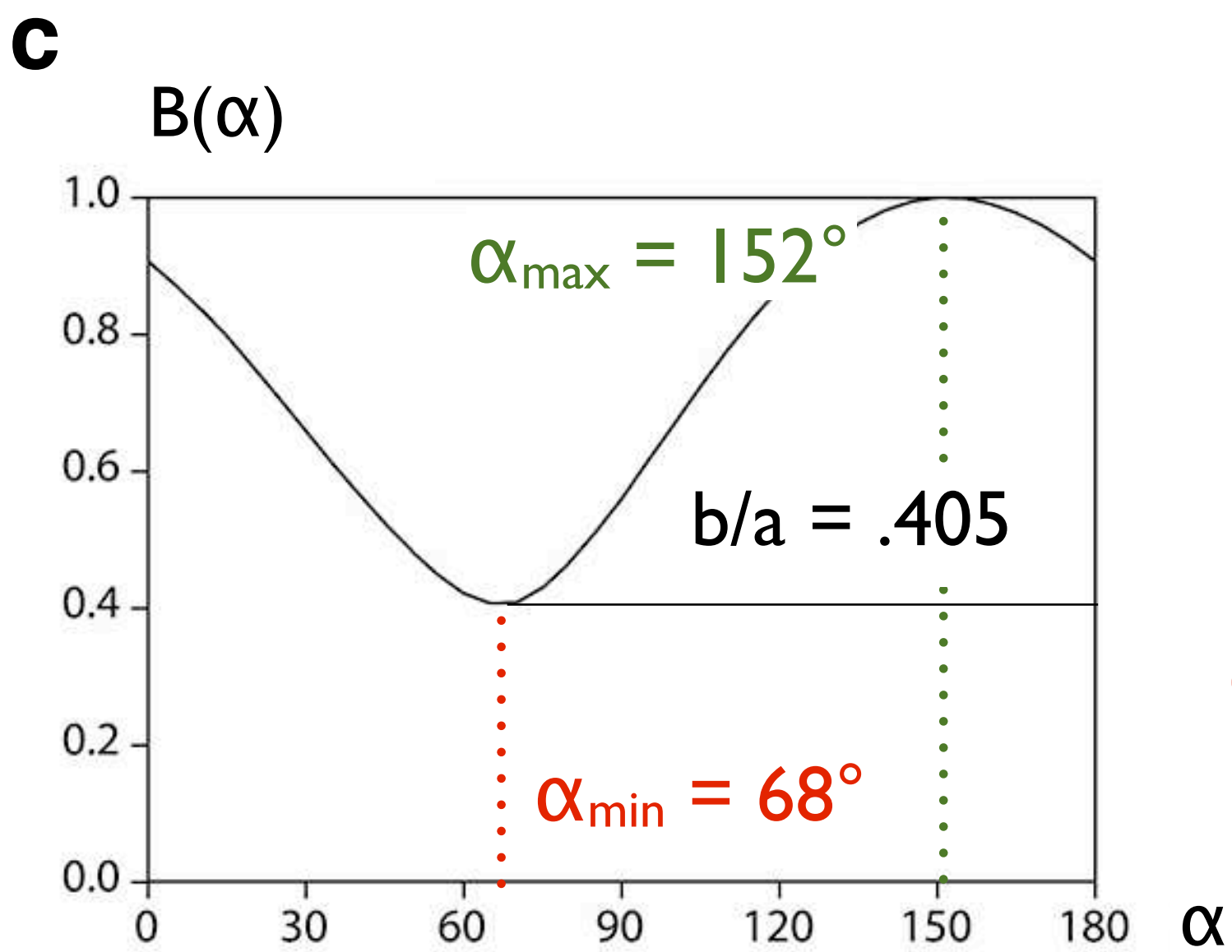
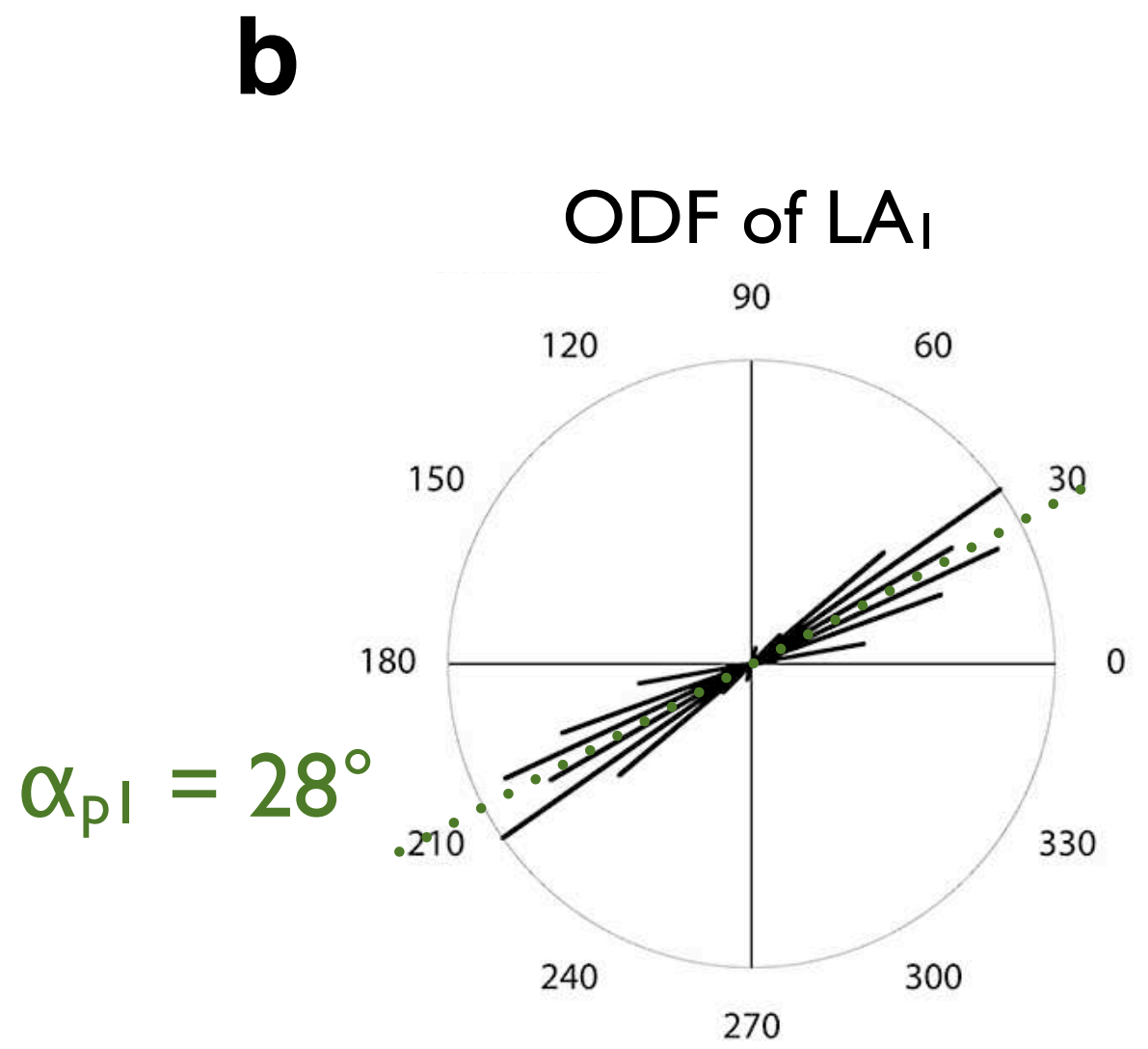
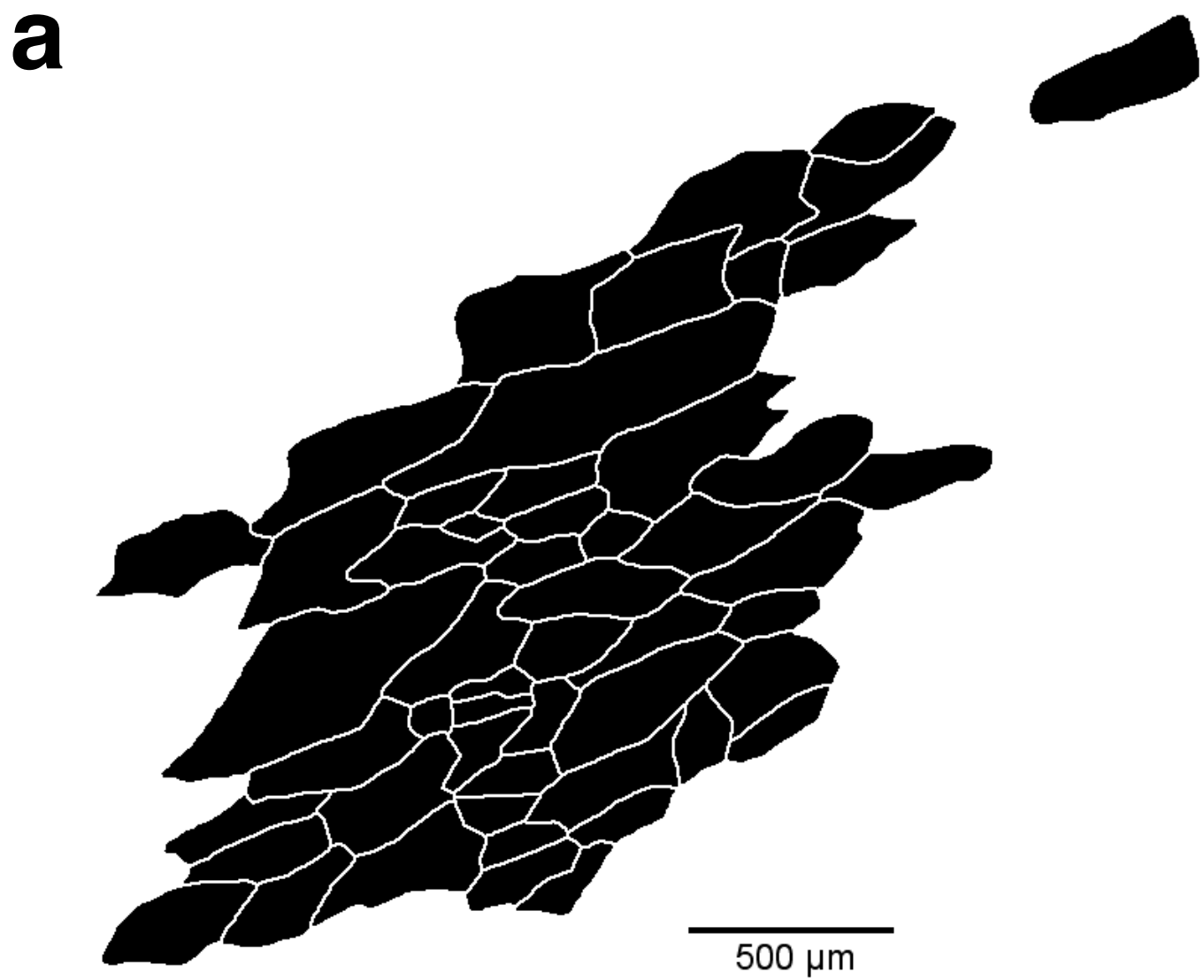


Figure 14.13

PAROR analysis of an experimentally sheared marble.

(a) Bitmap of fabric (prepared from sample CTI);

(b) projection curve $B(\alpha)$ of CTI.cor.scm;

(c) rose diagrams of long axes of particles (5° resolution) using LA_1 axes (longest projections of particles);

(d) same as (c) using LA_2 axes (= projections normal to the shortest projection).

The bulk preferred orientations, α_{p1} (green) and α_{p2} (red), calculated from α_{max} and α_{min} , respectively, are superposed on the rose diagrams. (The exact values for b/a , α_{p1} and α_{p2} were derived from analyses made with 1° increment of rotation).

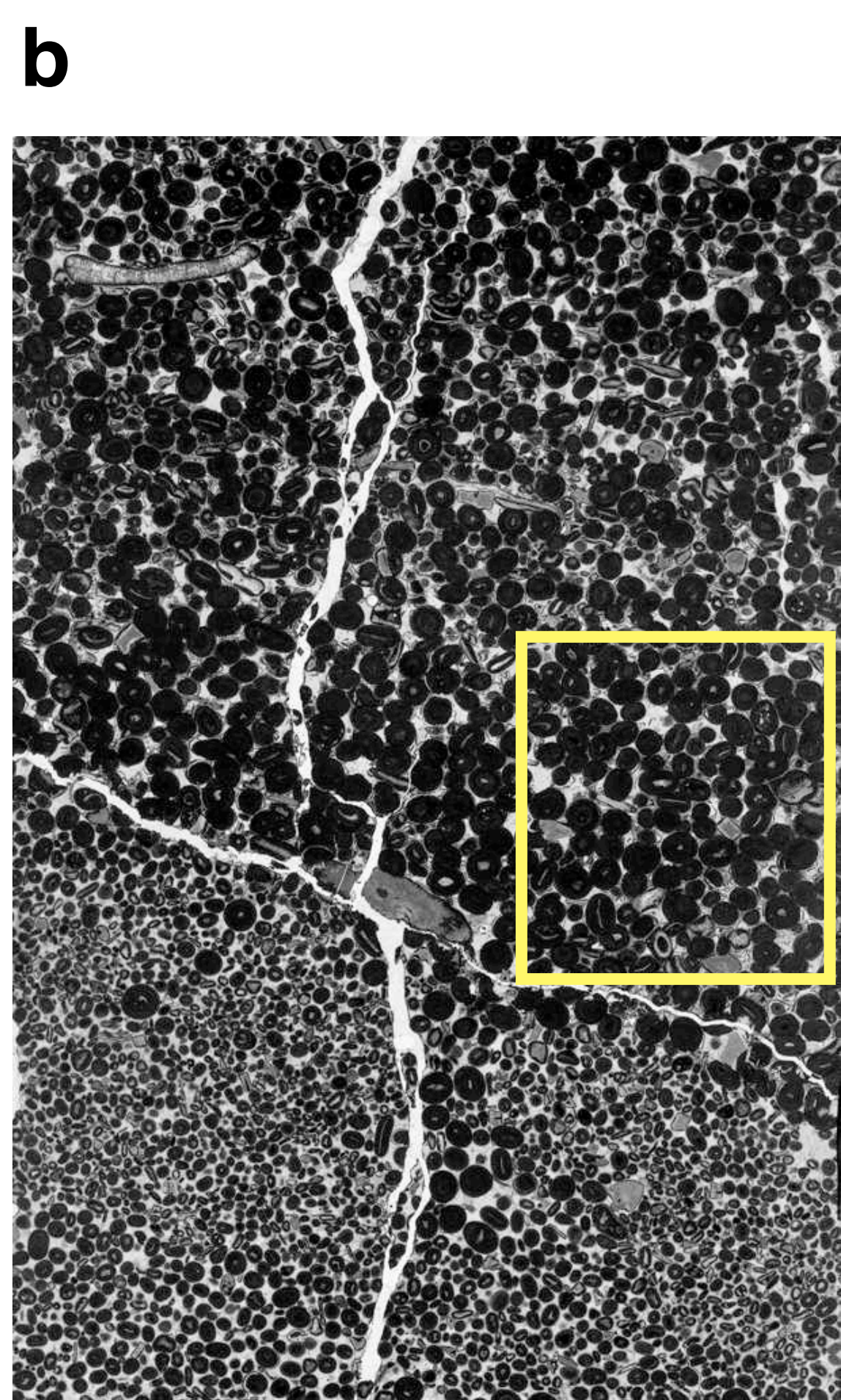


Figure 14.14

Over-packed oolitic limestone with grain-to-grain pressure solution contacts.

(a) Analyzed area of thin section, inverted contrast, showing packing of ooids.

(b) entire thin section (area shown = $21 \cdot 32 \text{ mm}^2$), transmitted light; rectangle denotes analyzed area. (Sample courtesy Samuel Mock).

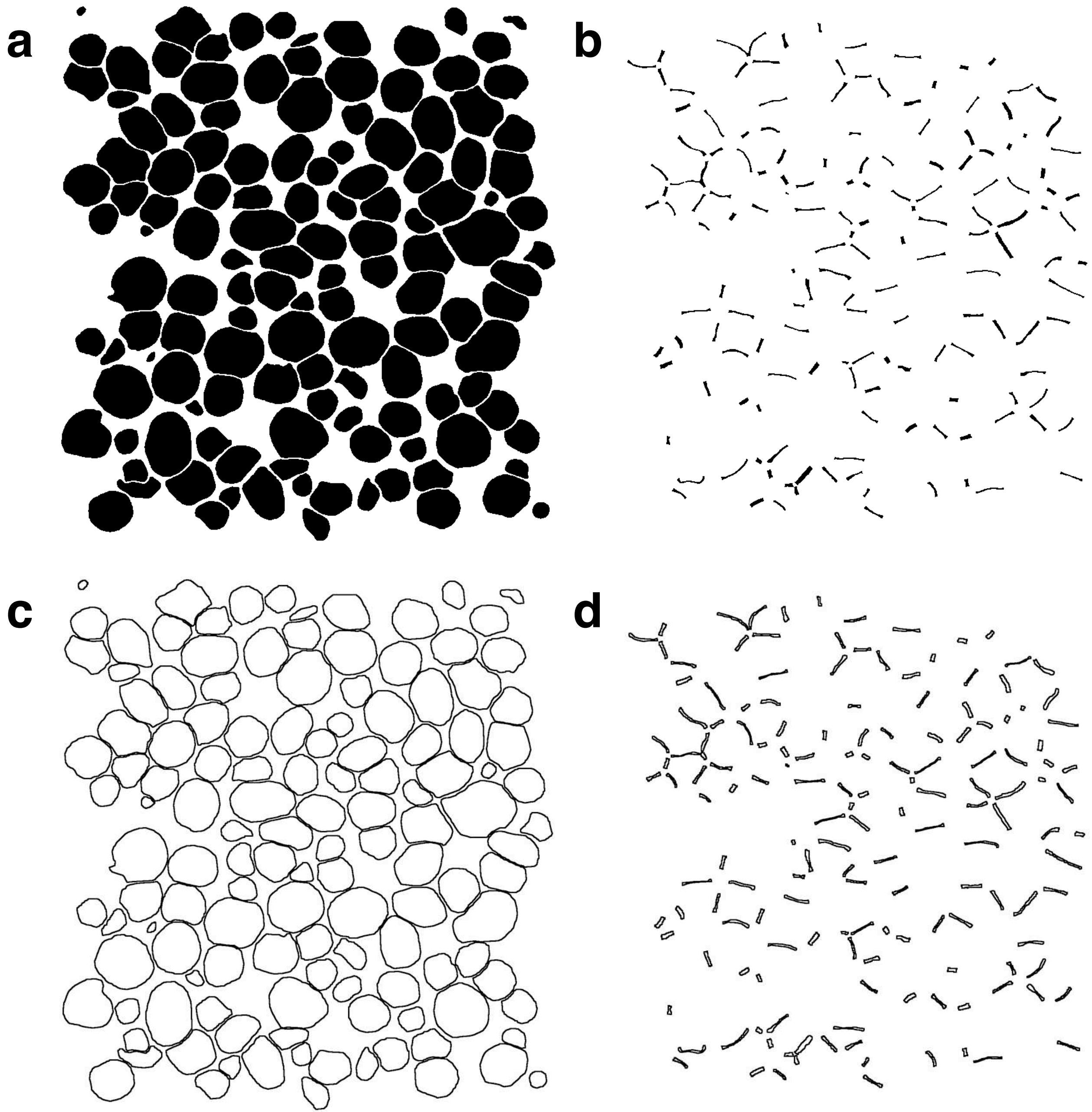


Figure 14.15

Ooides and pressure solution grain-to-grain contacts.

(a) Bitmap of ooides (b) bitmap of contact surfaces;

(c) outlines of ooides (d) outlines of contact surfaces.

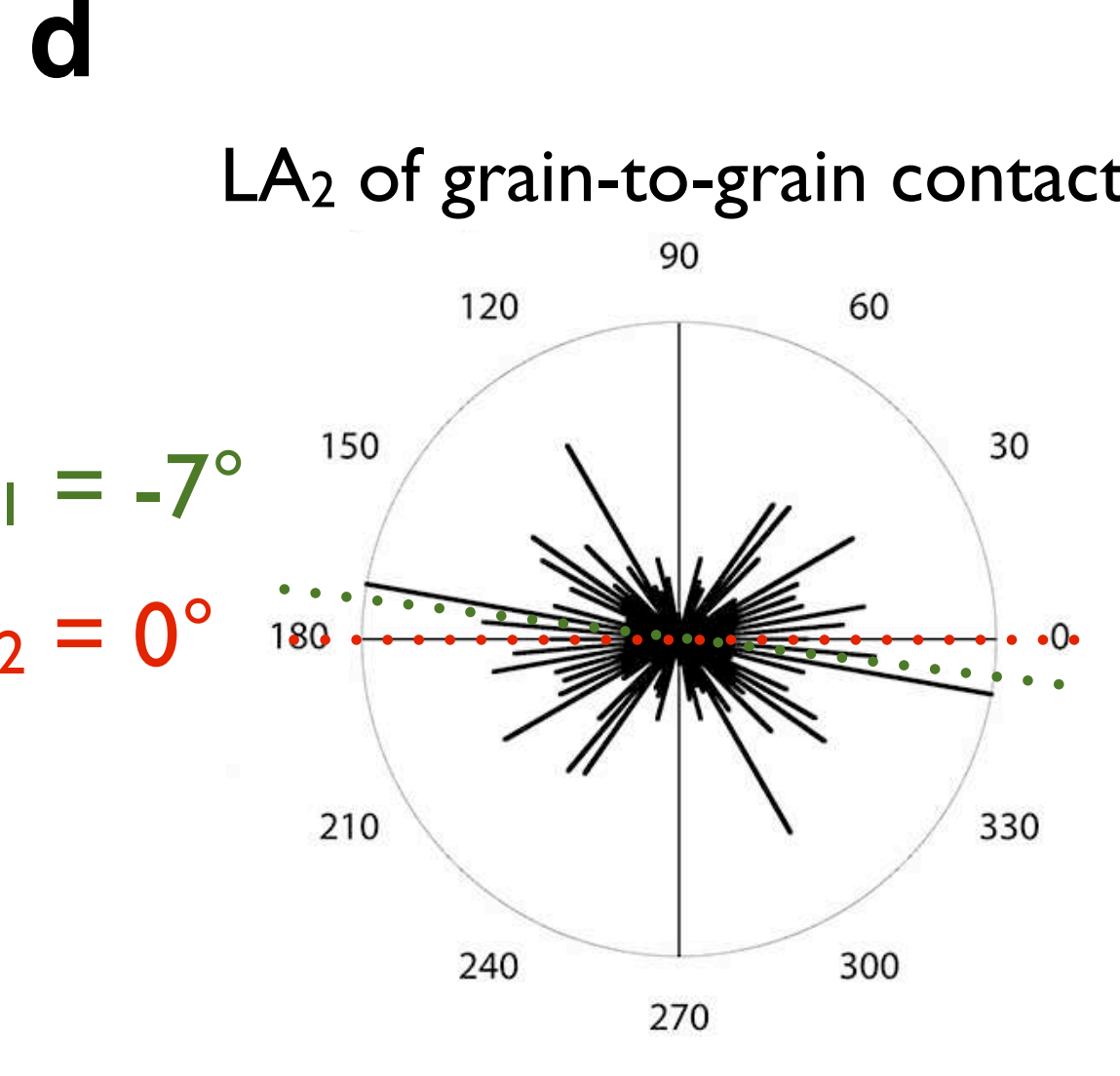
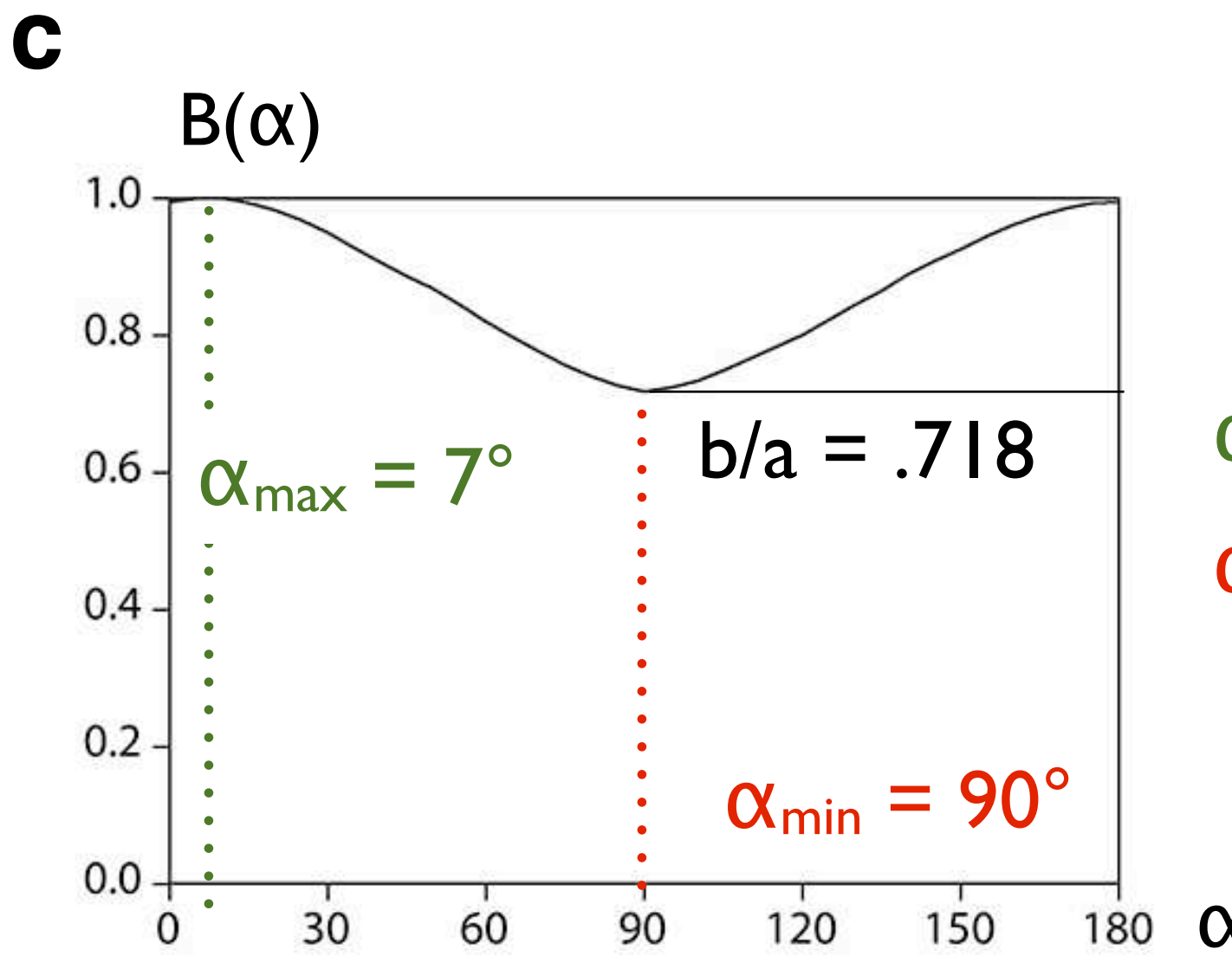
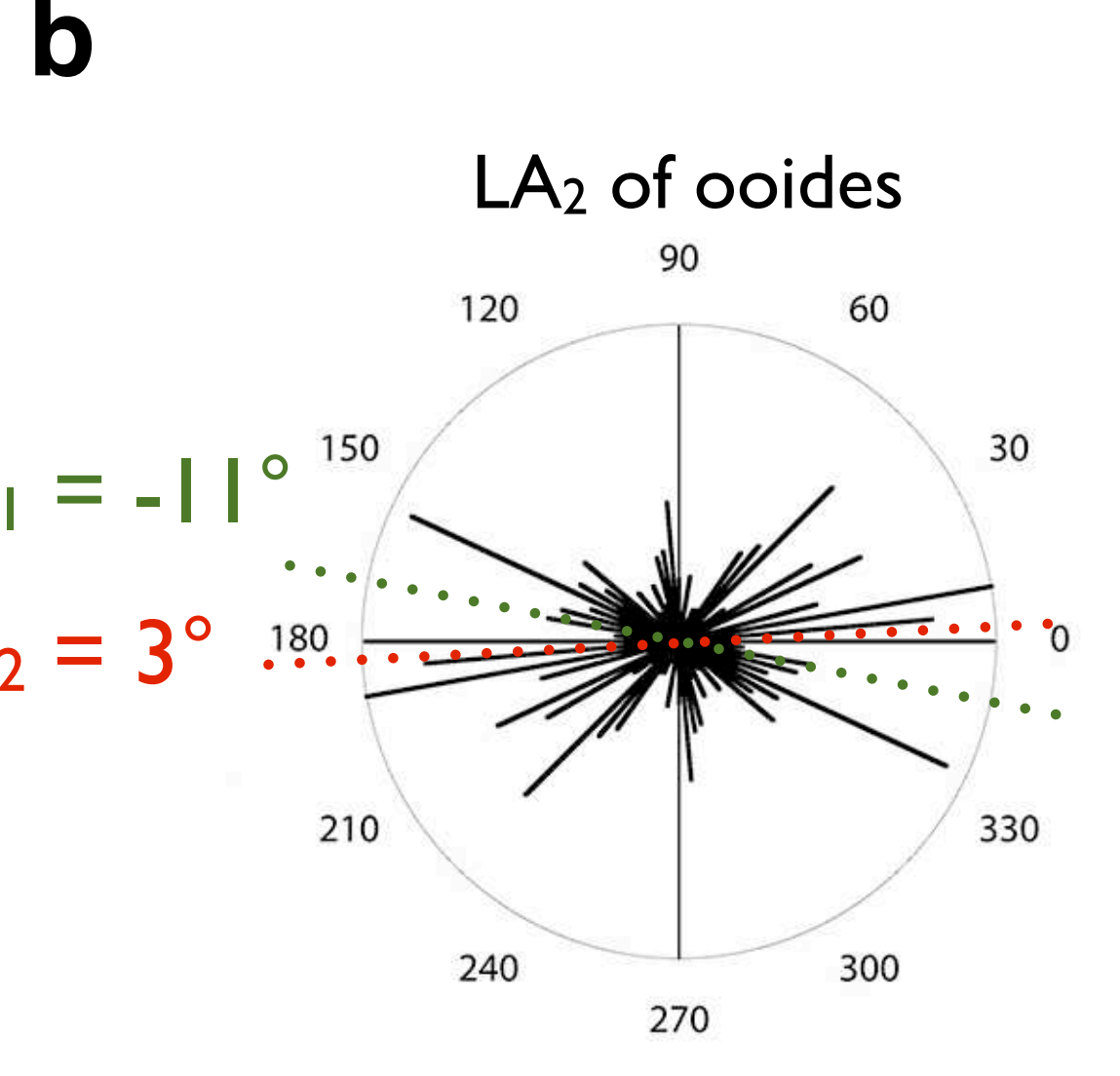
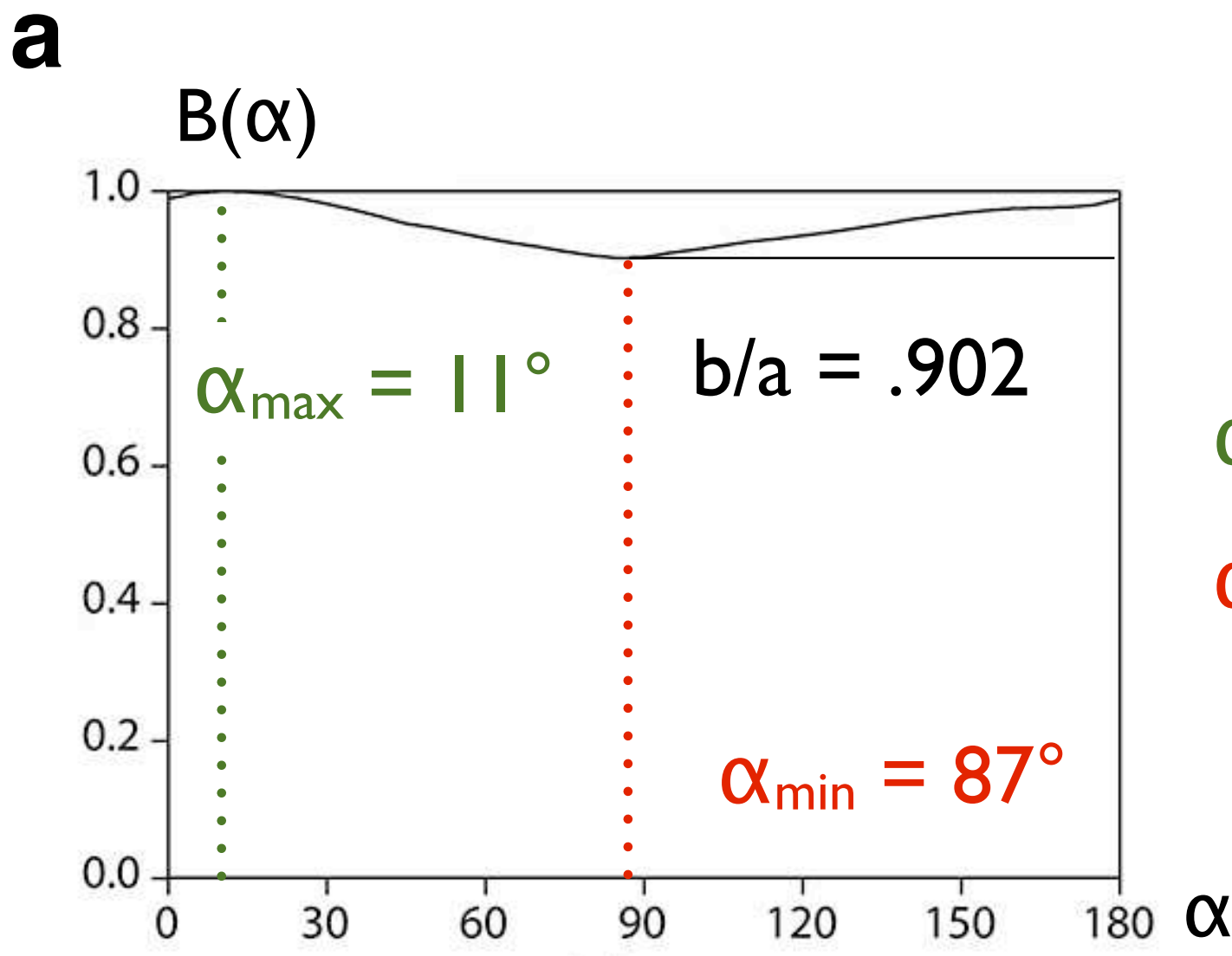
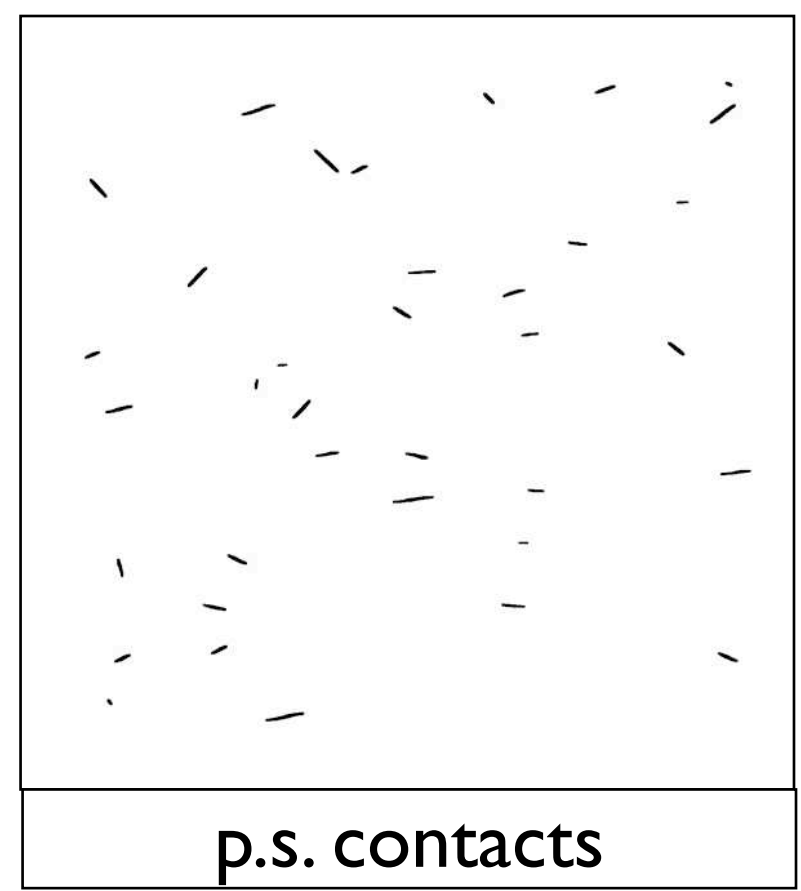
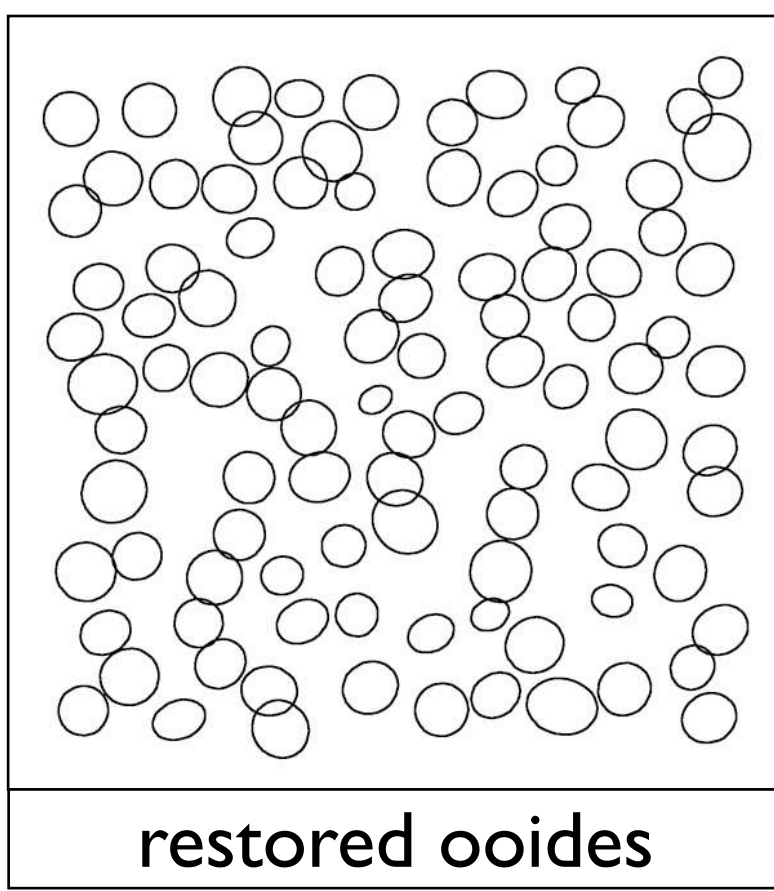
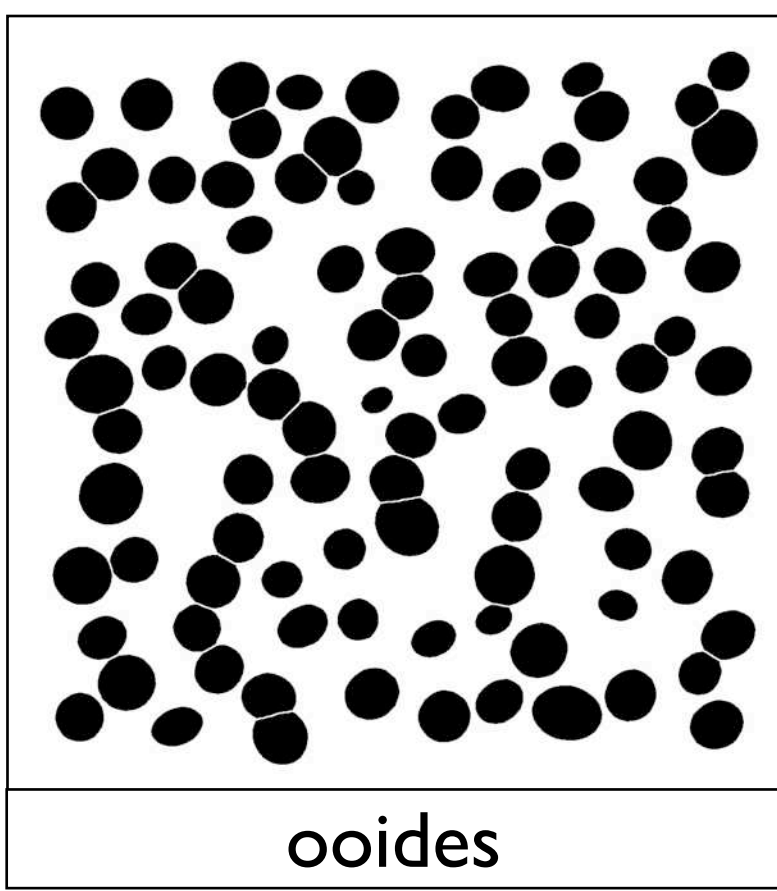
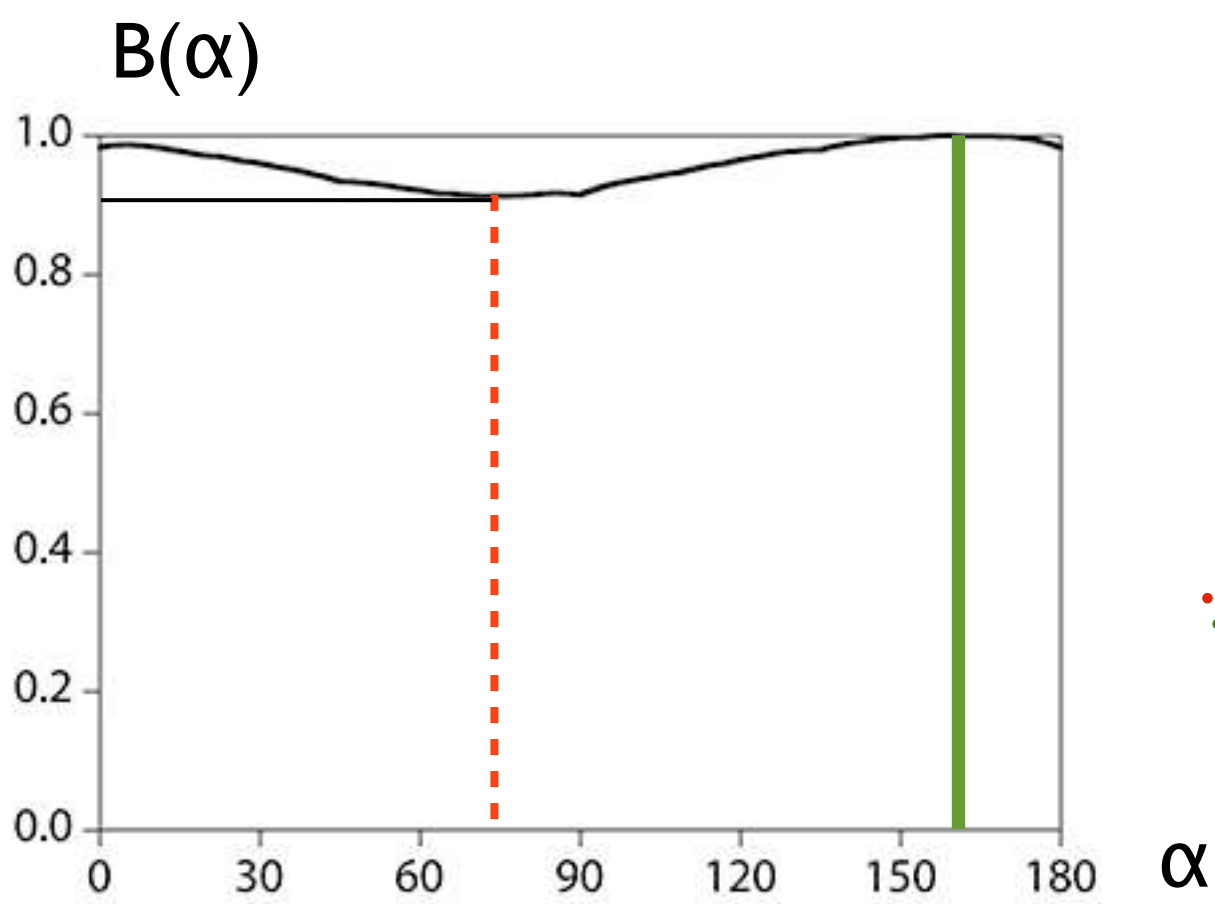
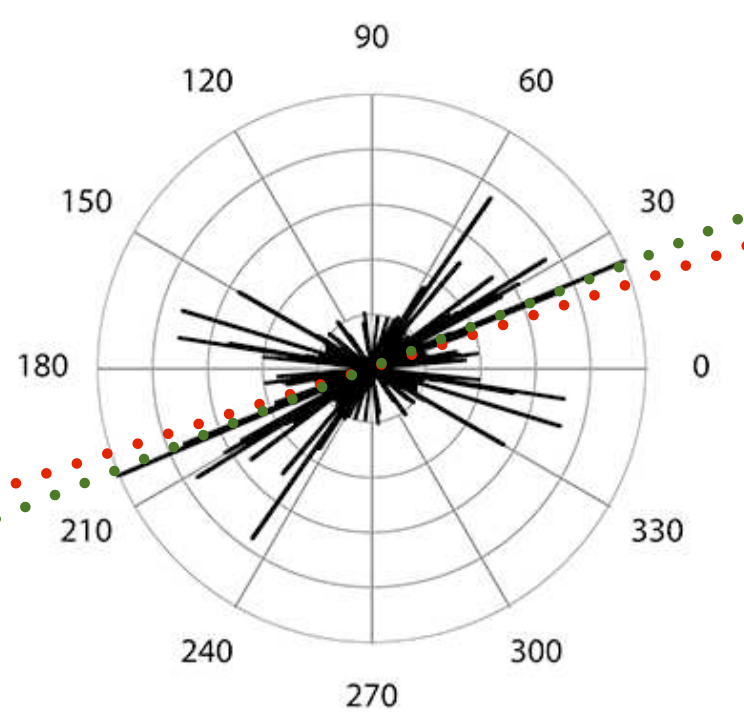


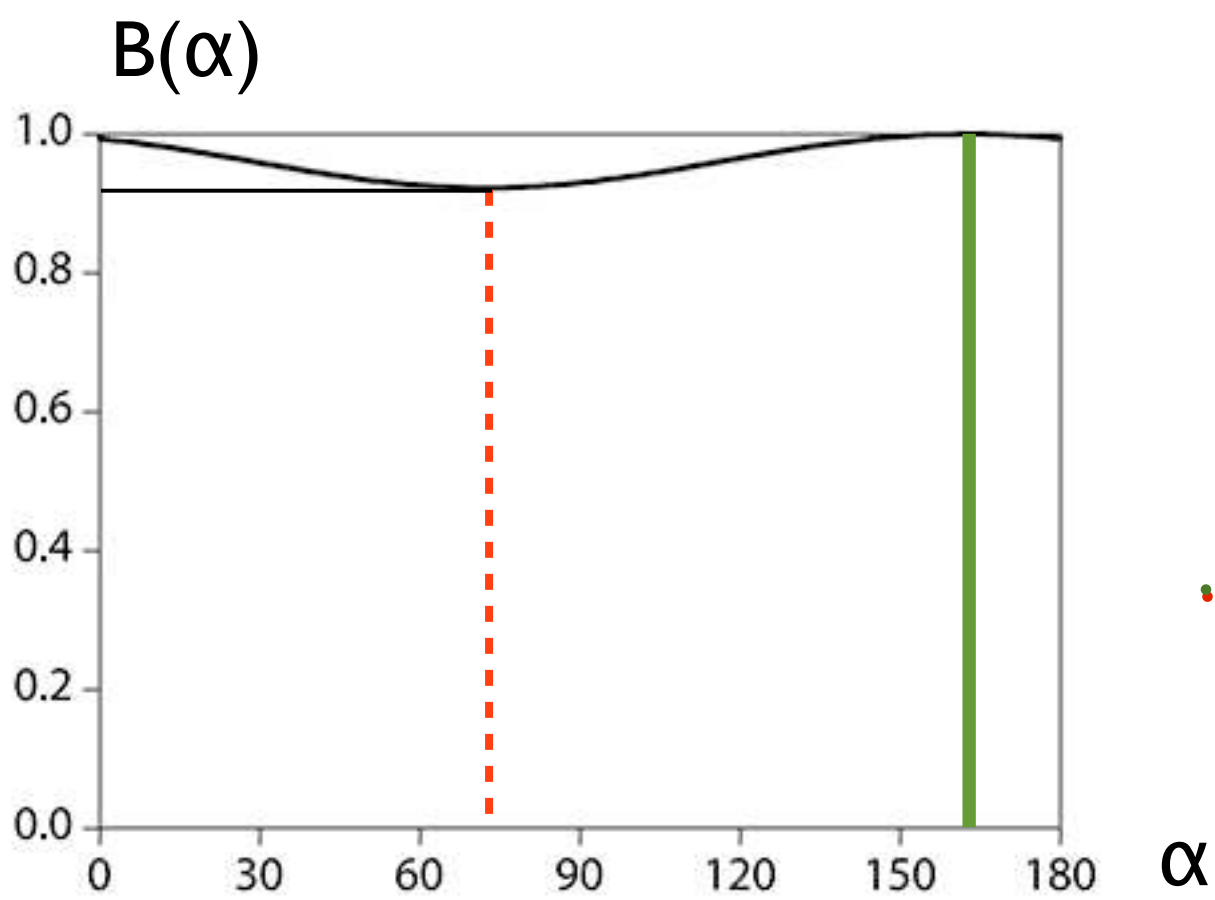
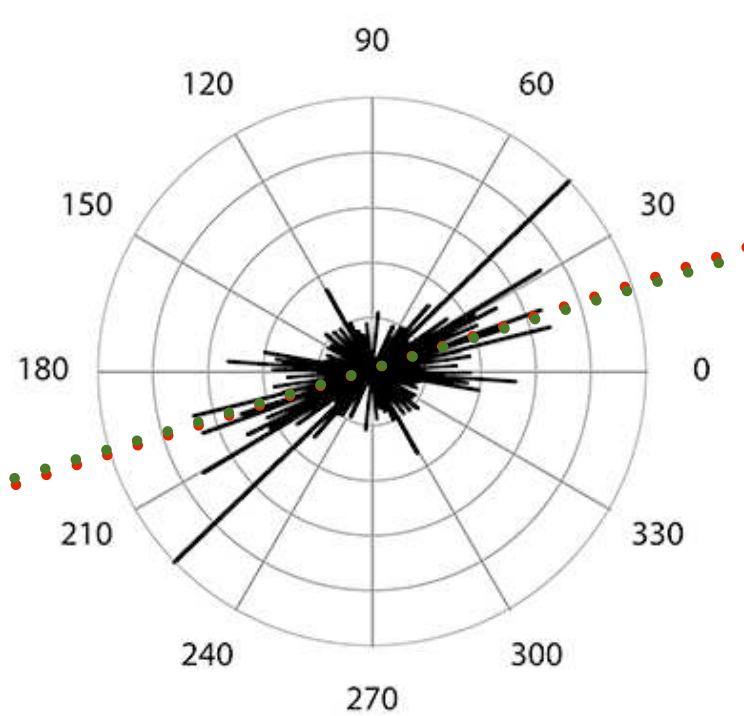
Figure 14.16
 PAROR analysis of ooides and grain-to-grain contacts.
 (a) projection curve $B(\alpha)$ of the ooides (outlines in file oo.cor.scm);
 (b) projection curve $B(\alpha)$ of contact areas (outlines in ps.cor.scm);
 (c) rose diagrams of long axes of ooides (results file oo.cor.r05, 5° resolution);
 (d) rose diagrams of long axes of contact areas (result file ps.cor.r05, 5° resolution): LA₂ = long axes defined by the projection normal to the shortest projection.
 Superposed in (c) to (d) are the preferred orientations, α_{p1} (red) and α_{p2} (green), derived from α_{\max} and α_{\min} ; the exact values for b/a , α_{\min} and α_{\max} were derived from analyses made with 1° increment of rotation.

a**b** LA_1 of ooides

$\alpha_{p1} = 22^\circ$

$\alpha_{p2} = 18^\circ$

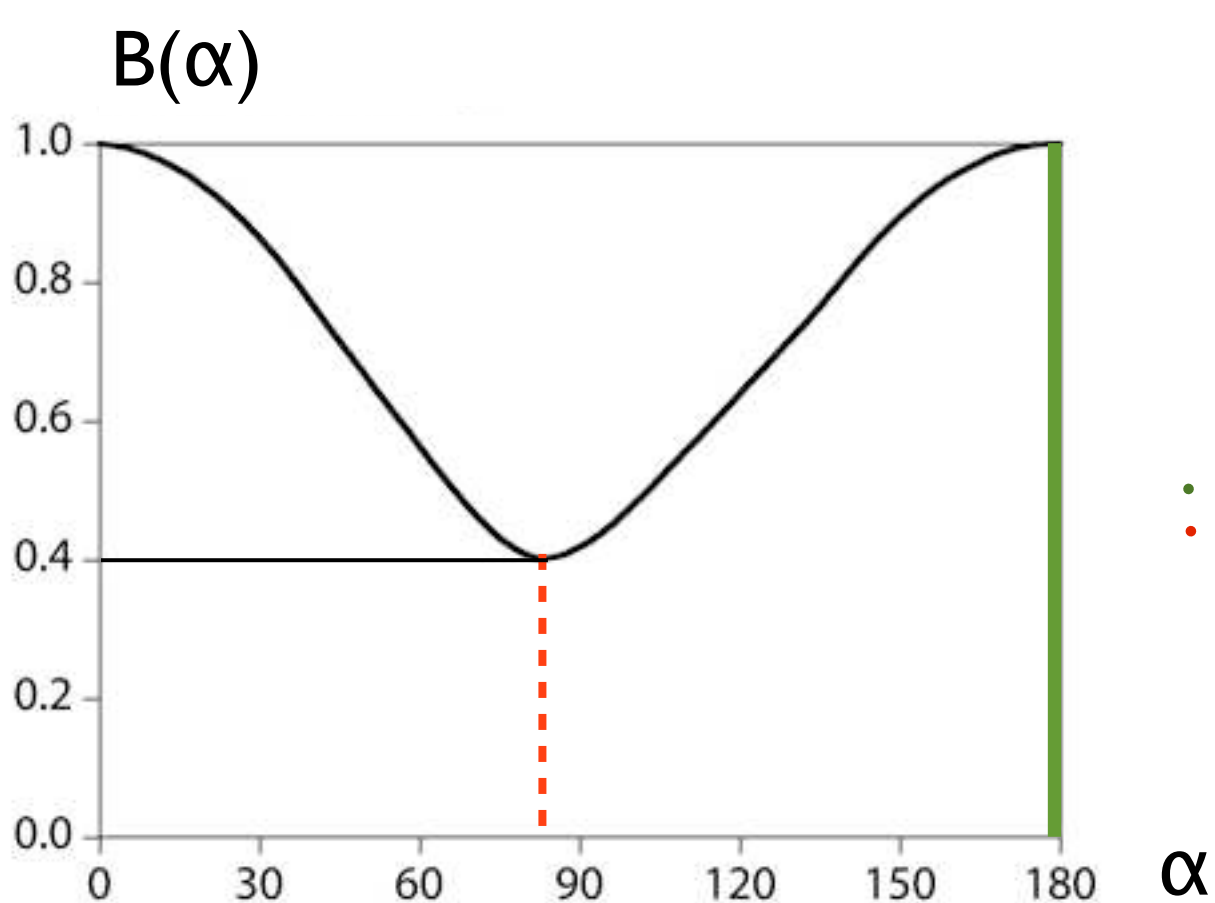
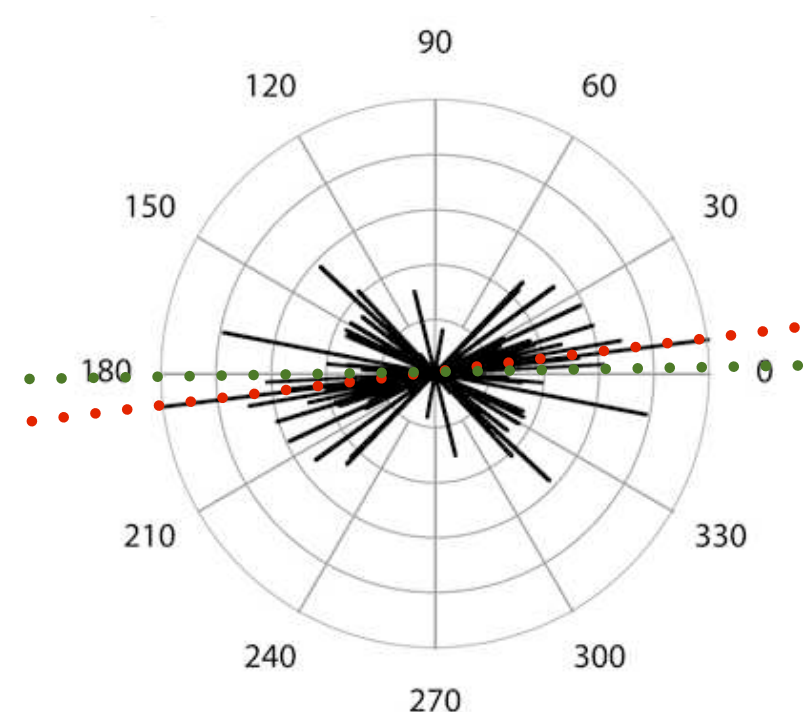
$b/a = 0.91$

c LA_1 of restored ooides

$\alpha_{p1} = 17^\circ$

$\alpha_{p2} = 18^\circ$

$b/a = 0.92$

d LA_1 of p.s. contacts

$\alpha_{p1} = 1^\circ$

$\alpha_{p2} = 7^\circ$

$b/a = 0.40$

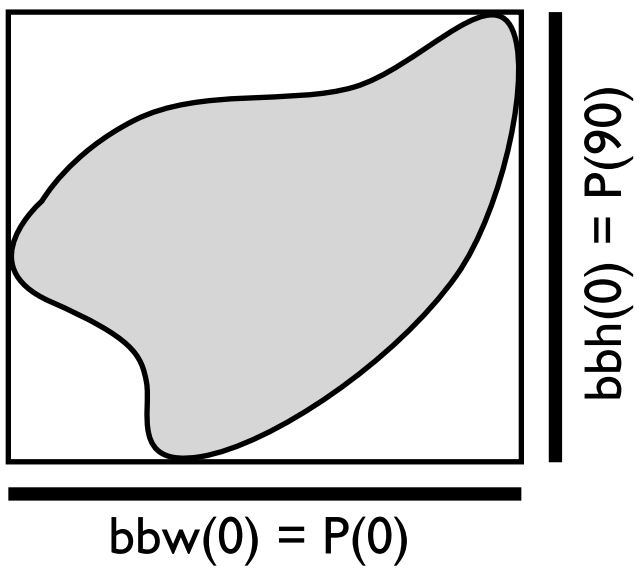
Figure 14.17

Restoring outlines - recreating 'fossil' fabrics.

(a) From left to right: Bitmap of present day ooides with pressure solution grain-to-grain contact; outlines of restored ooides; outlines of pressure solution contacts;

(b) to (d) PAROR analysis of present day ooides (b), of restored ooides (c) and of pressure solution contacts (d); particle projection, $B(\alpha)$, is shown on left; ODF of long axes, LA_1 , on right; preferred orientations, α_{p1} (green) and α_{p2} , (red) are superposed on rose diagram, the value for $b/a = B(\alpha)_{\min} / B(\alpha)_{\max}$, is indicated.

rotation = 0°



rotation = 50°

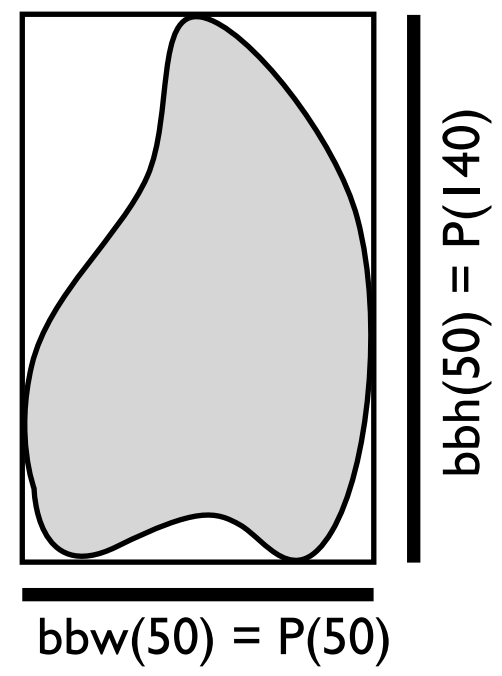


Figure 14.18

Concept of bounding box.

At any given orientation of the outline, the width of the bounding box, $bbw(\alpha)$, corresponds to the length of projection on the x-axis, i.e., to $P(\alpha)$; the height of the bounding box, $bbh(\alpha)$, to the projection on the y-axis, i.e., to $P(\alpha + 90^\circ)$.

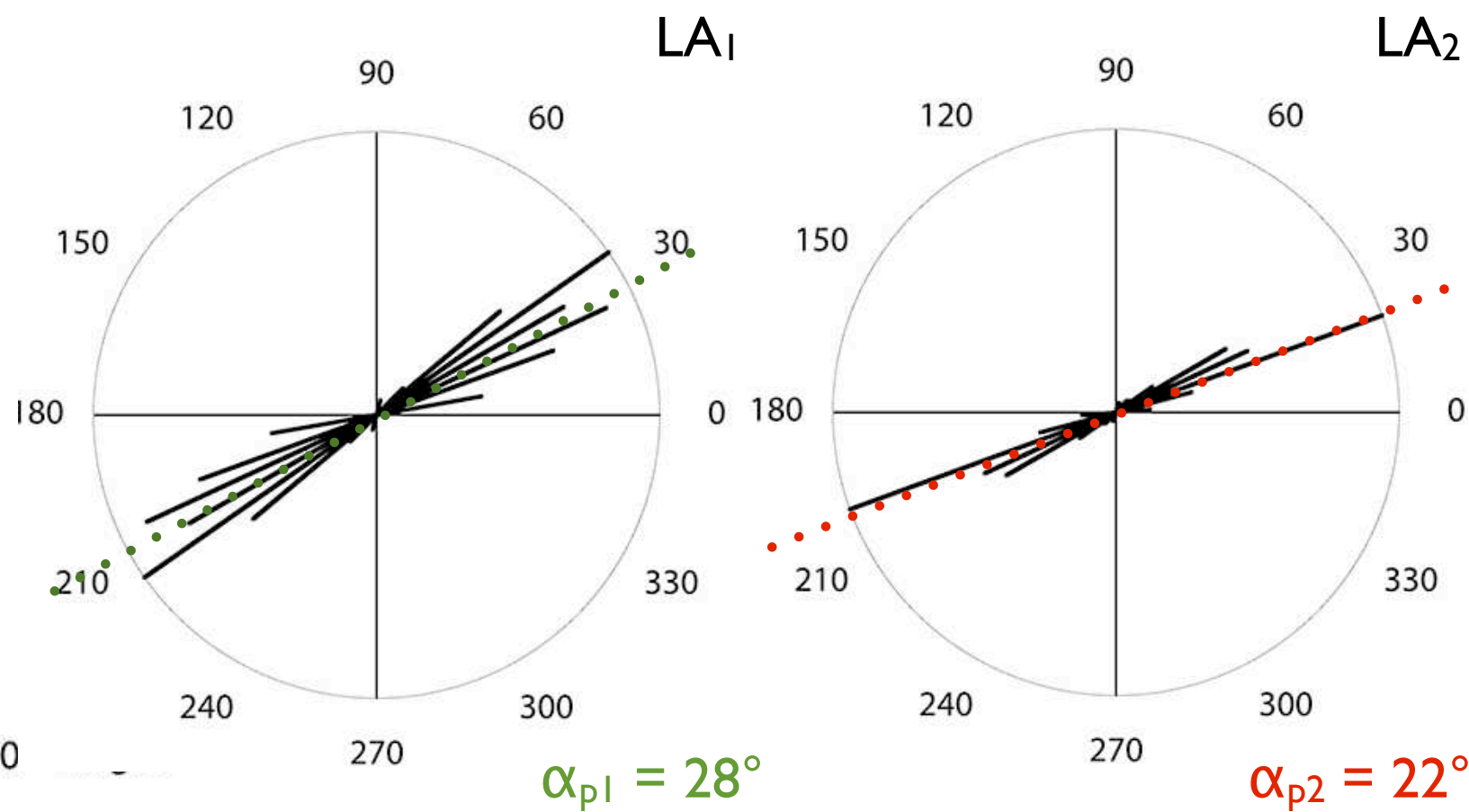
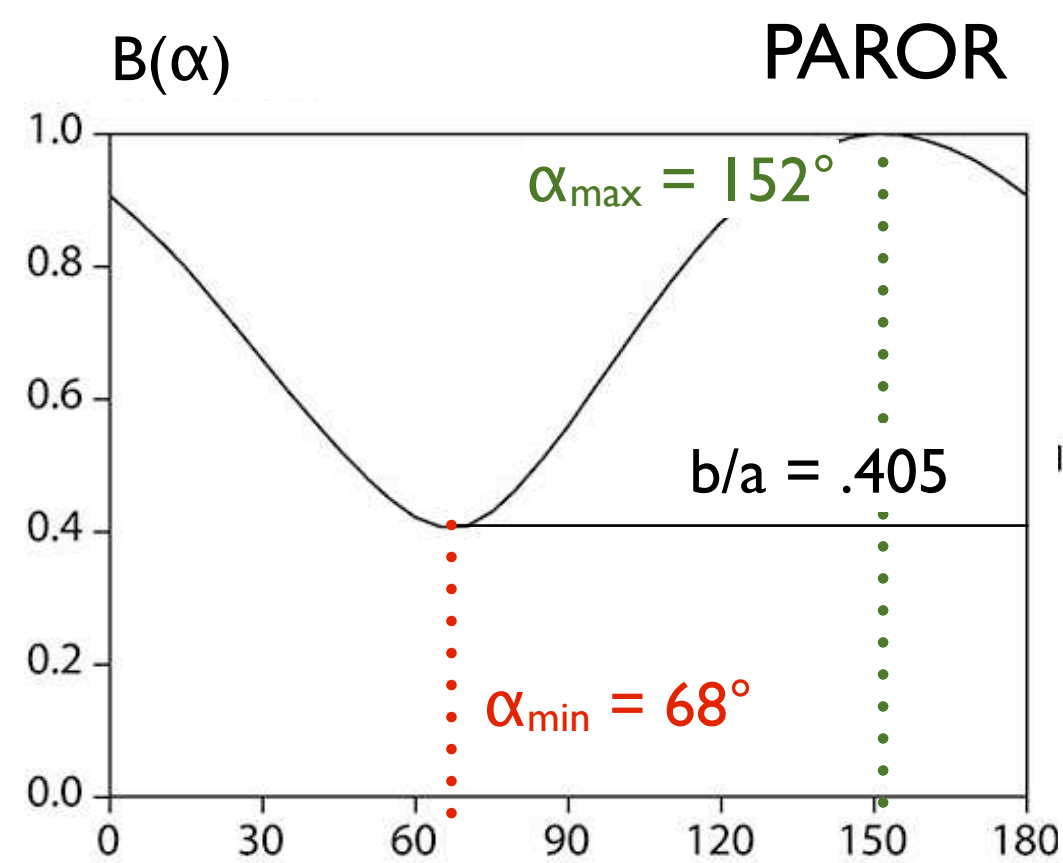
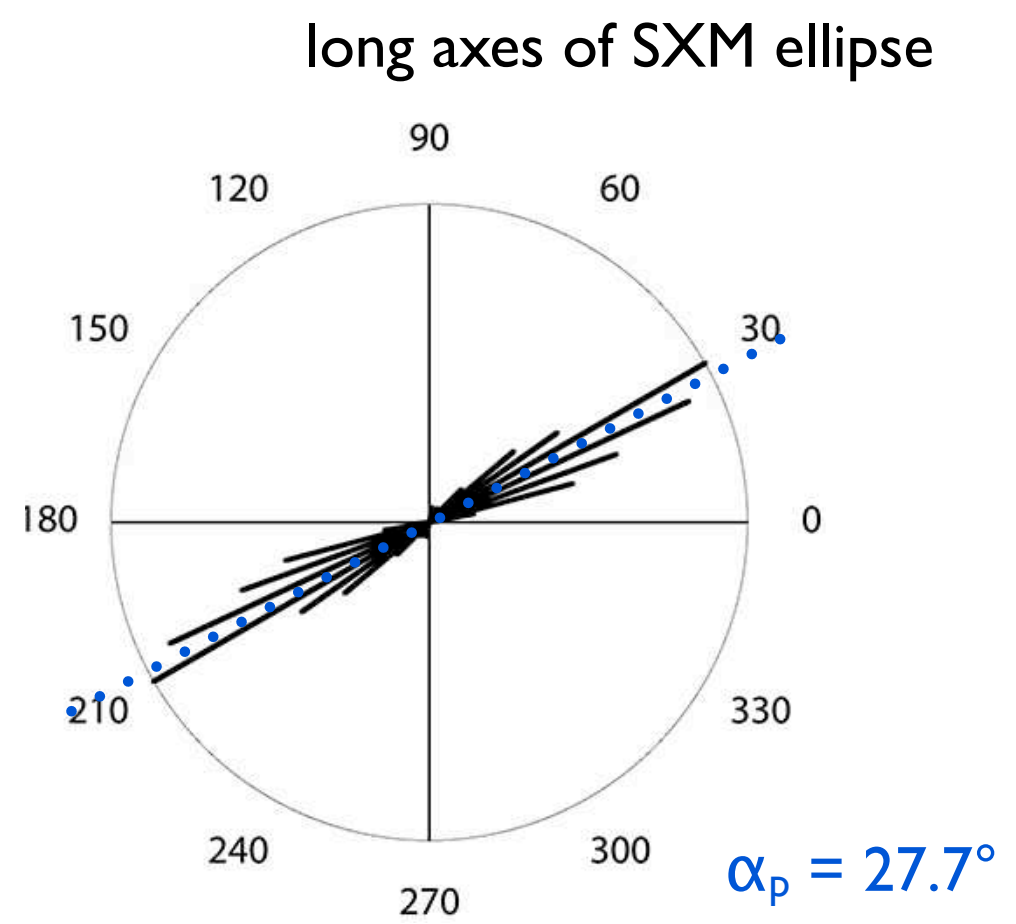
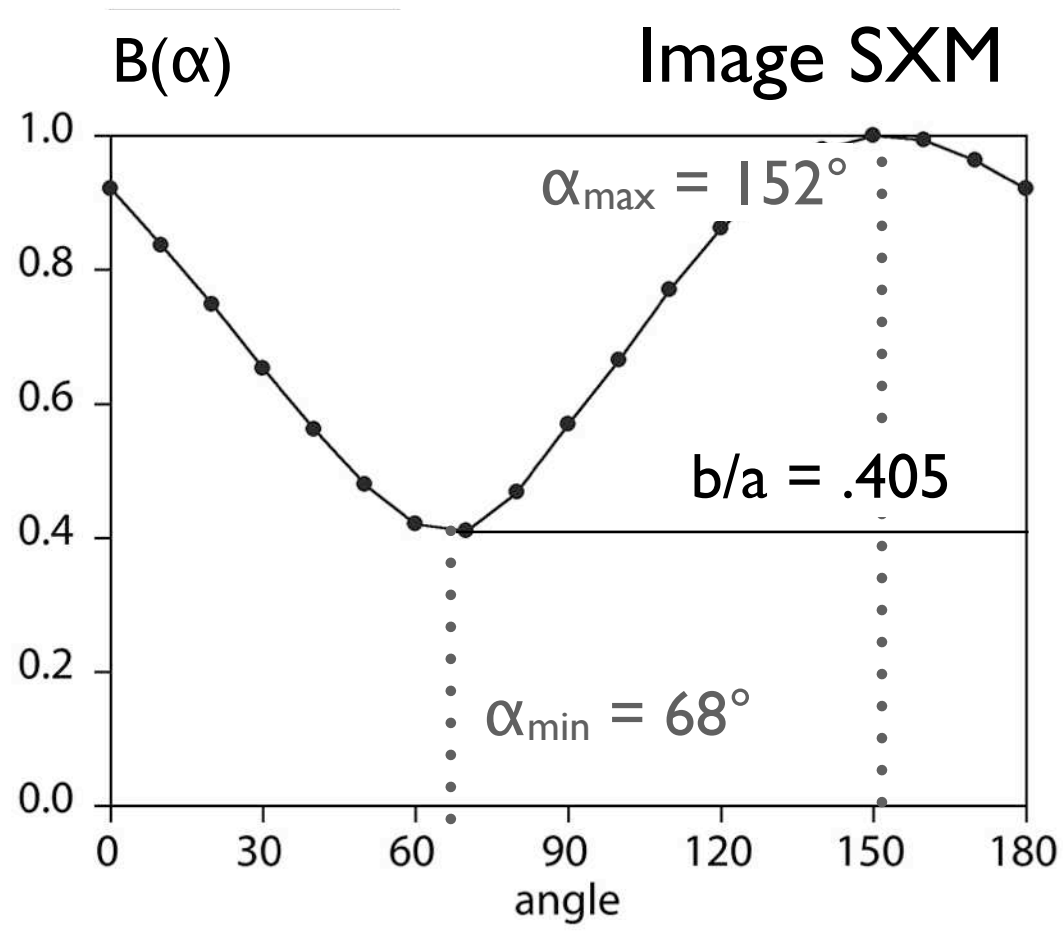


Figure 14.19

Comparison of PAROR and bounding box results for sample CT1 (Figure 14.13).

Left: projection curves $B(\alpha)$: top: calculated using bounding boxes of Image SXM at 10° intervals; bottom: using PAROR projections at 1° interval (bottom);

Right: rose diagrams of long axes of particles (5° resolution): top: ODF of the long axes of SXM best-fit ellipses; bottom: ODF of the longest projections LA_1 and projections normal to the shortest LA_2 .

All rose diagrams are length weighted; in blue: average orientation of the long axes of the SXM ellipses; in green and red: the bulk preferred orientations, α_{p1} and α_{p2} , calculated from α_{\max} and α_{\min} , respectively, and superposed on the rose diagrams; the exact values for b/a , α_{p1} and α_{p2} were derived from analyses made with 1° increment of rotation.